

Haptic Sensors and Interfaces for Interactive Dexterous Robotic Telemanipulation

Emil M. Petriu, FIEEE
*School of Electrical Engineering and Computer Science
University of Ottawa, Canada*

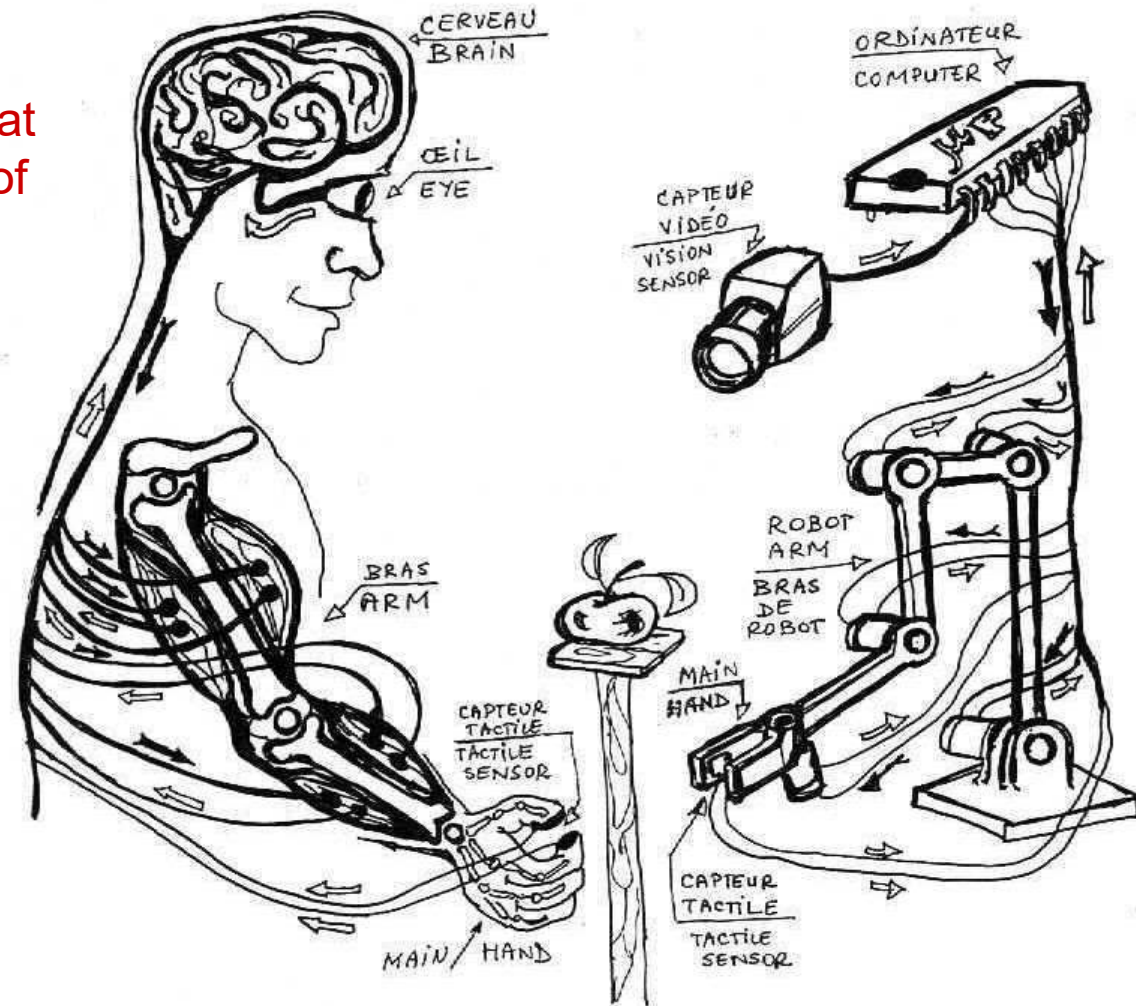
“In a way, **touch can be constructed as the most reliable of the [human] sensor modalities**. When the senses conflict, touch is usually the ultimate arbiter. ... Touch sensations can arise from stimulation anywhere on the body’s surface. Indeed, the **skin can be characterized as one large receptor surface for the sense of touch**. ... The English neurologist H. Jackson paid homage to the wonderful and complex abilities of the *human hand* by calling it *the most intelligent part of the body*. The skin on the human hand contains thousands of **mechanoreceptors** (sensitive to mechanical pressure of deformation of the skin), as well as a **complex set of muscle to guide the fingers** as they explore the surface of an object. The mechanoreceptors play a key role in analyzing object detail such as texture; the muscles make their big contribution when grosser features such as size, weight, and shape are being analyzed. But, whether exploring gross or small details, the **hand and the finger pads convey the most useful tactile information about objects**. In this respect, the hand is analogous to the eye’s fovea, the region of retina associated with keen visual acuity. There is, however, a flaw in this analogy: fovea vision is most acute when the eye is relatively stationary, but **touch acuity is best when the fingers move of the object of regard**” [from [R. Sekuler, R. Balke, *Perception*, 2nd edition, McGraw-Hill, NY, 1990, Chapter 11. Touch, pp. 357-383].

The time has now arrived to add biology - and more specifically, human anatomy, physiology and psychology - to the scientific sources of knowledge for engineers to develop a *new, bio-inspired, generation of intelligent machines*.

Advocating this emergent trend, this presentation will discuss haptic sensors and human interfaces, and intelligent control algorithms for human-like multi-finger robot hands able to dexterously explore, grasp, and in-hand manipulate objects.

These emergent technologies will allow the development of a new generation of remotely controlled intervention robots able to interactively perform complex tele-manipulation operations in high-risk operational environments like nuclear power stations, underwater, highly infectious rooms, robotic surgery, or war zones.

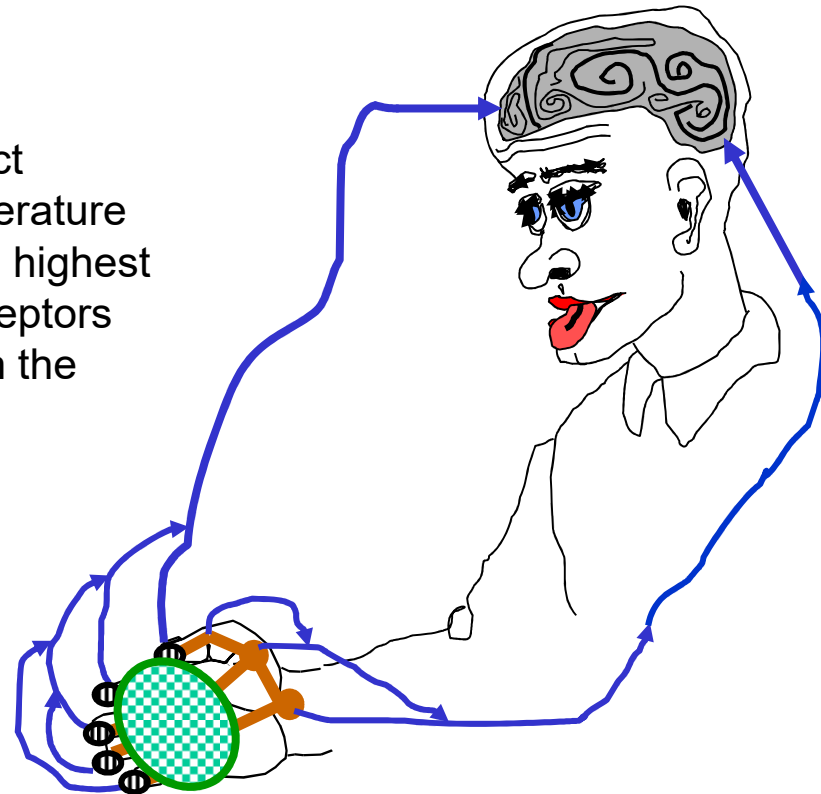
Robot haptic perception mechanisms that emulate those of the humans.



Human Haptic Perception

Human haptic perception is the result of a complex dexterous manipulation act involving two distinct components:

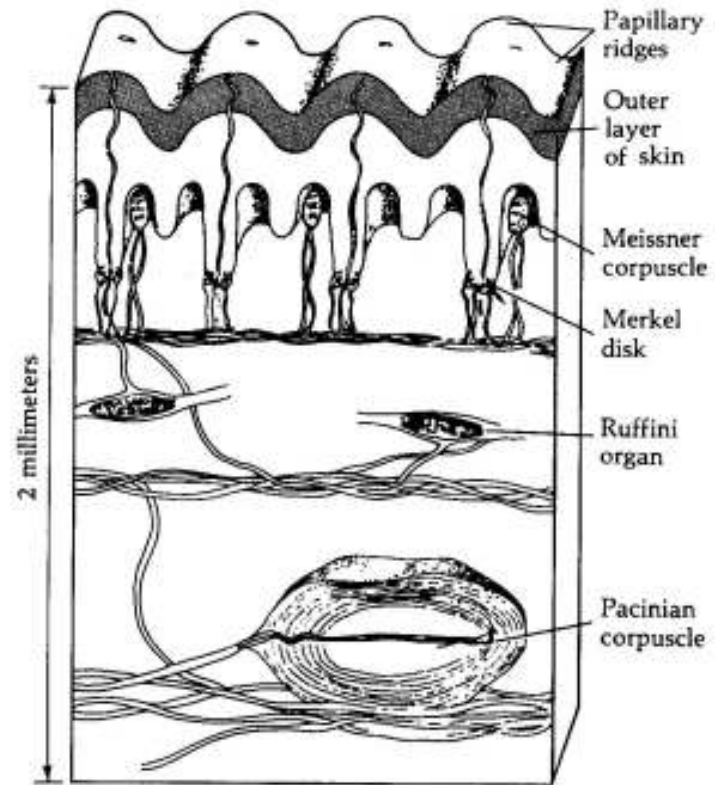
- (i) **cutaneous** information from skin mechanoreceptors which provide about the geometric shape, contact force, elasticity, texture, and temperature of the touched object surface. The highest density of cutaneous mechanoreceptors is found in **fingerpads** (and also in the **tongue**, the **lips**, and the foot). Force information is mostly provided by **muscle**, **tendon** and **bone joint** proprioceptors;
- (ii) **kinesthetic** information about the positions and velocities of the **kinematic structure (bones and muscles)** of the hand



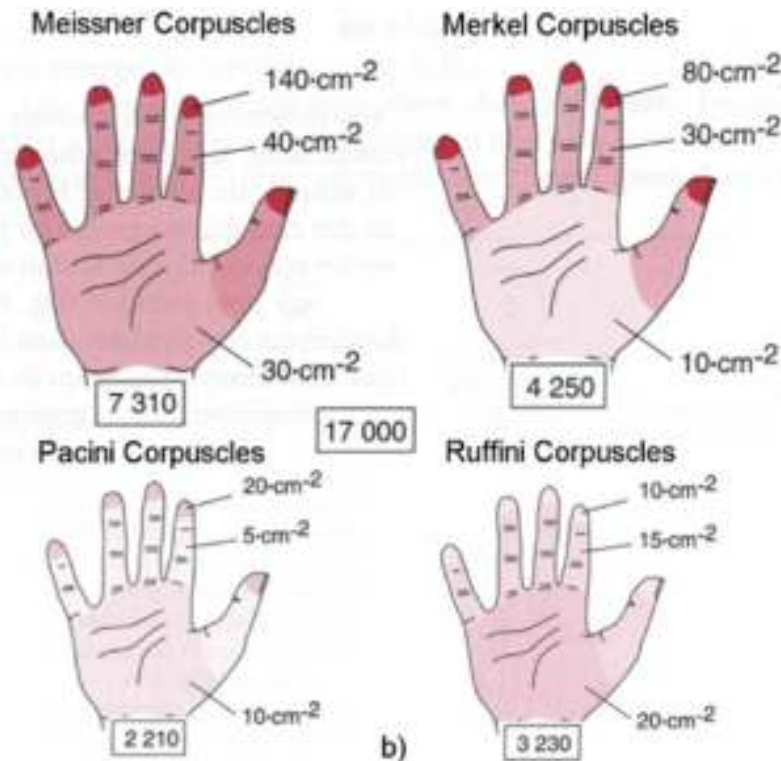
Cutaneous tactile mechanoreceptors

- 40 % are **Meissner's corpuscles** sensing velocity and movement across the skin;
- 25% are **Merkel's disks** which measure pressure and vibrations;
- 19% are **Rufini corpuscles** sensing skin shear and temperature changes.
- 13 % are **Pacinian corpuscles** (buried deeper in the skin) sensing acceleration and vibrations of about 250 Hz;

[from G. Burdea and Ph. Coiffet, *Virtual Reality Technology*, 2nd edition, Wiley, New Jersey, 2003]



[from [R. Sekuler, R. Balke, *Perception*, 2nd edition, McGraw-Hill, NY, 1990]

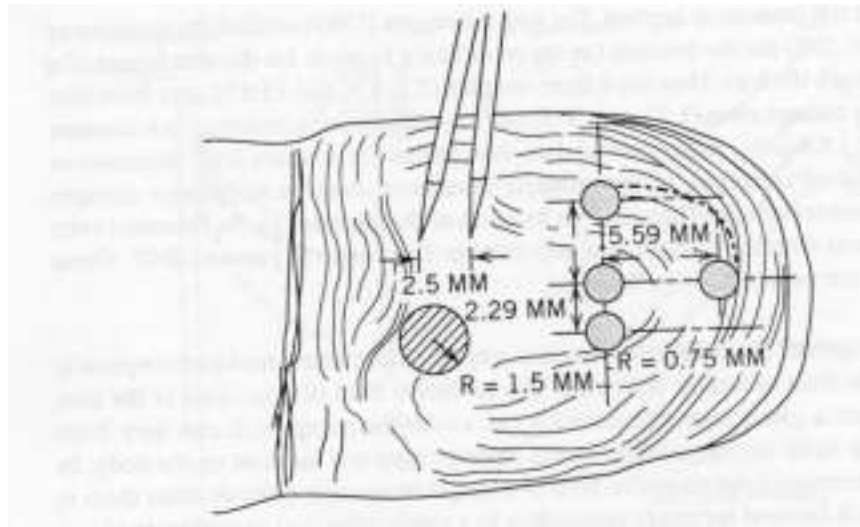


Tactile sensing receptor densities in the human hand

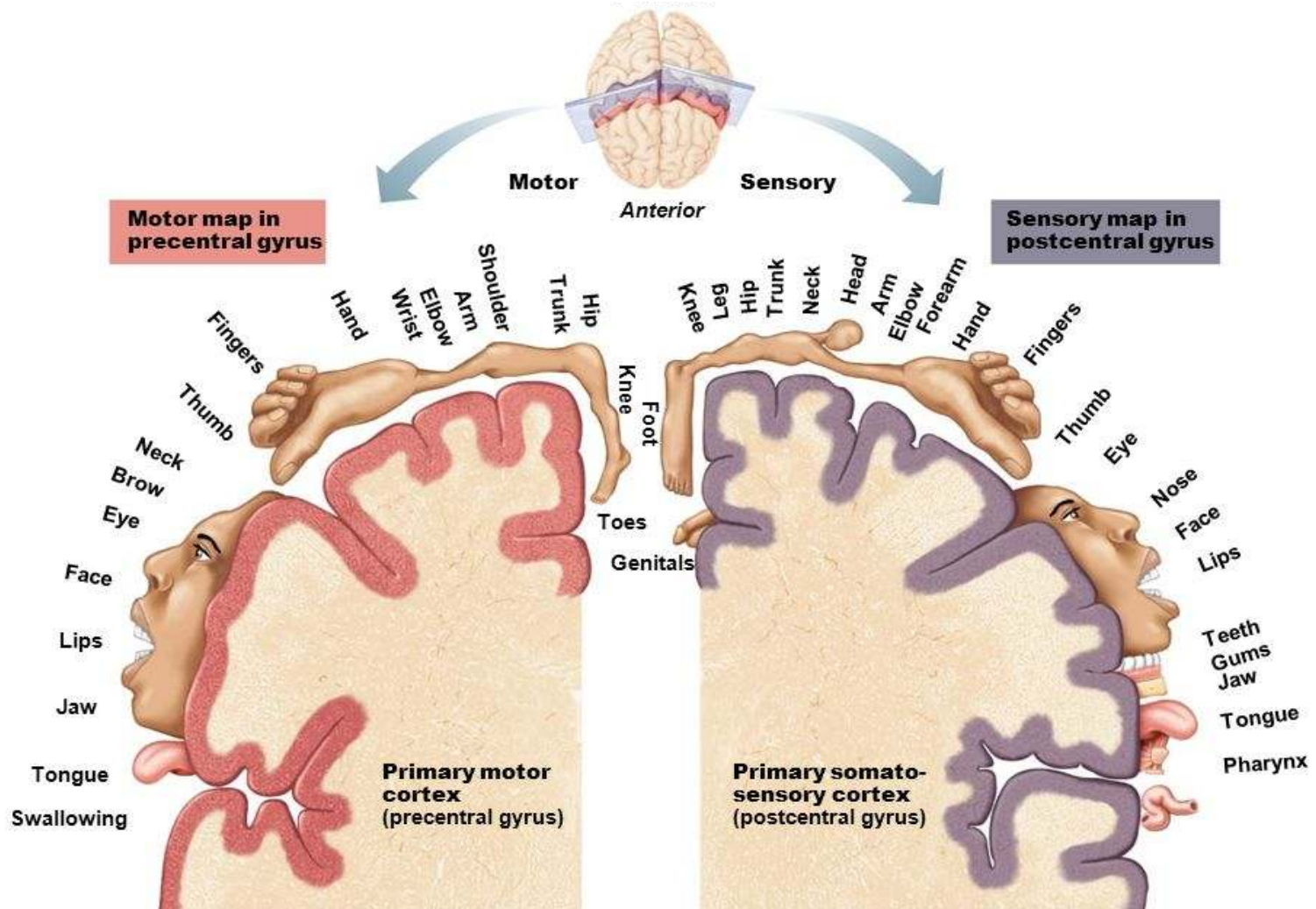
[from R Johansson & A Vallbo, "Tactile Sensory Coding in the Glabrous Skin of the Human Hand," *Technical Innovations in Neuroscience -TINS*, Elsevier, pp. 27-32, Jan. 1983].

Spatial resolution

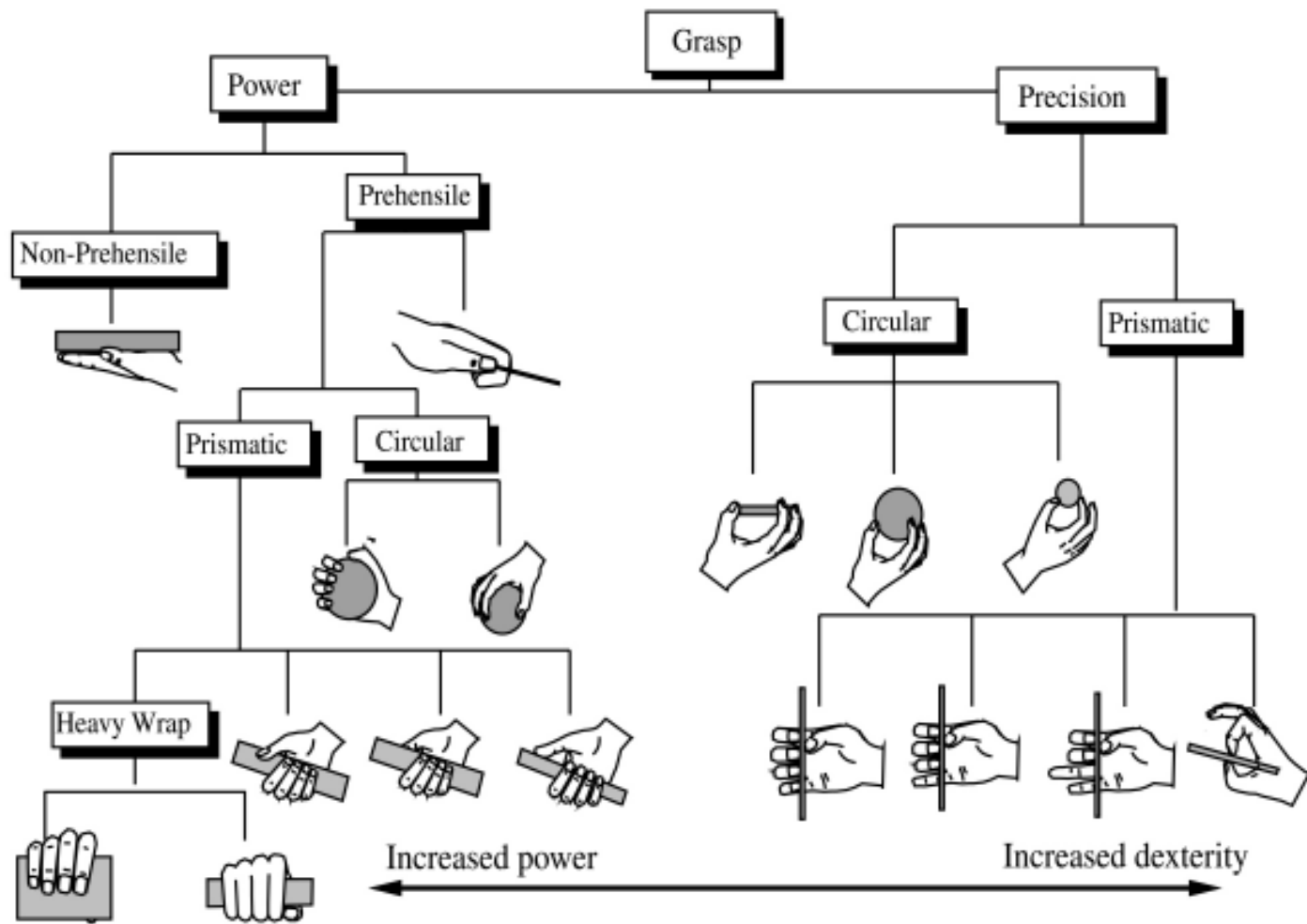
- If the sensor has a large receptive field – it has low spatial resolution (Pacinian and Ruffini)
- If the receptive field small - it has high spatial resolution (Meissner and Merkel)



Two-point limen test: 2.5 mm fingertip, 11 mm for palm, [from G. Burdea and Ph. Coiffet, *Virtual Reality Technology*, 2nd edition, Wiley, New Jersey, 2003]



Body maps in the motor cortex and somatosensory cortex of the cerebrum, [http://images.slideplayer.com/14/4280670/slides/slide_23.jpg].

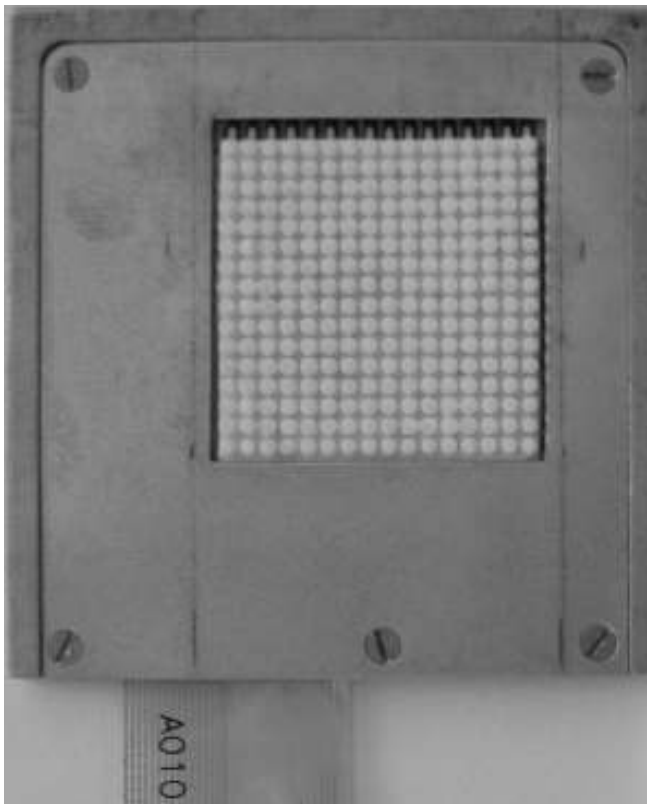


Human grasping configurations [from G. Burdea and Ph. Coiffet, *Virtual Reality Technology*, 2nd edition, Wiley, New Jersey, 2003]



**Tactile Sensing
Artificial Skin**

Tactile probe using an elastic overlay and 16-by-16 matrix of Force Sensing Resistors (FSR)



The **tabs of the elastic overlay** are arranged in a 16-by-16 array having a tab on top of each [Merkel's disk](#)-like matrix of **FSR elements** sensing sustained pressure and shapes.

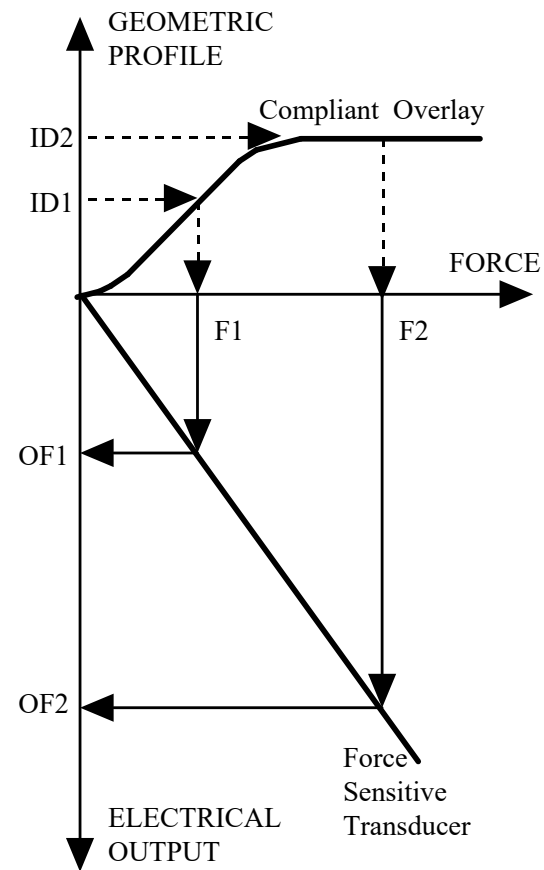
This tab configuration provides a *de facto* spatial sampling, which reduces the elastic overlay's blurring effect on the high 2D sampling resolution of the FSR sensing matrix.

[from S.K. Yeung, E.M. Petriu, W.S. McMath, D.C. Petriu, "High Sampling Resolution Tactile Sensor for Object Recognition," *IEEE Tr. Instr. Meas.*, Vol. 43, No. 2, pp.277-282, 1994.]

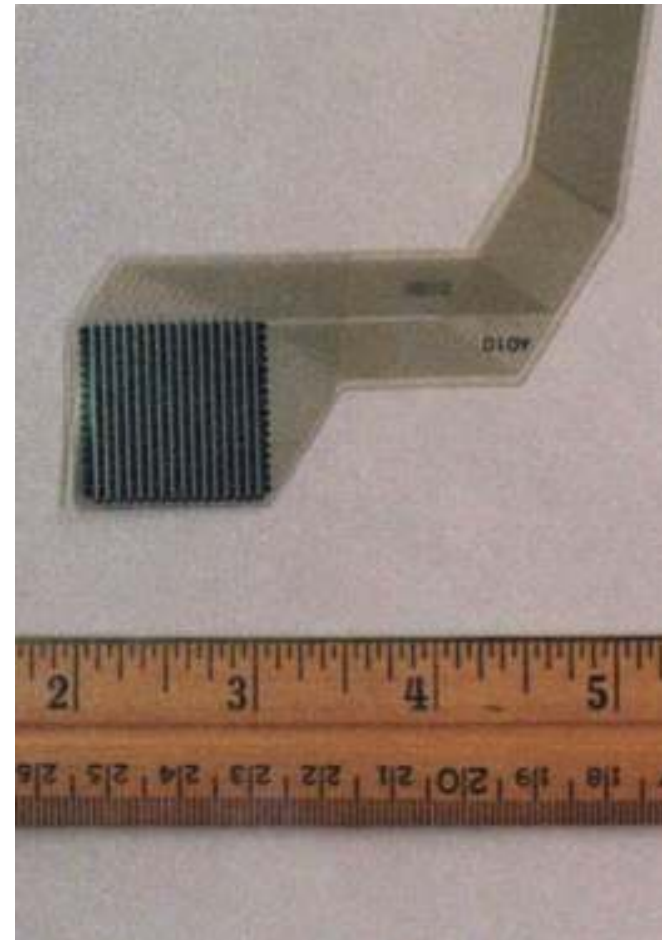
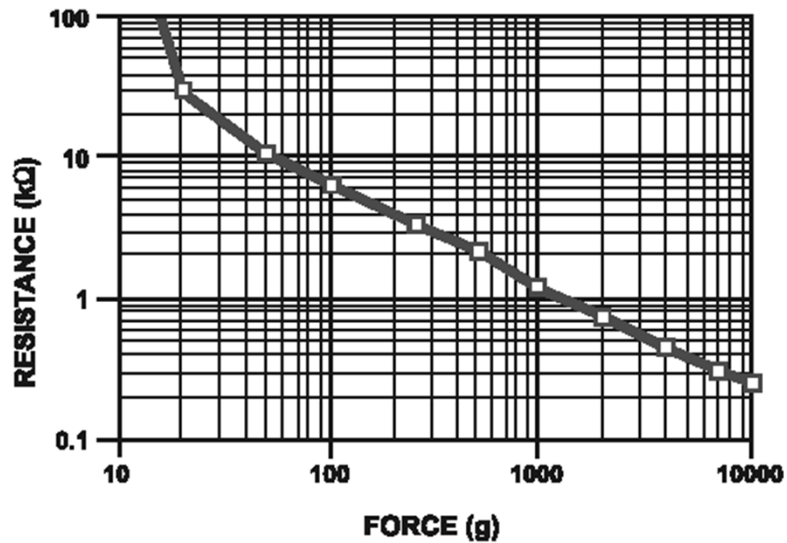
Tactile probing of object surfaces

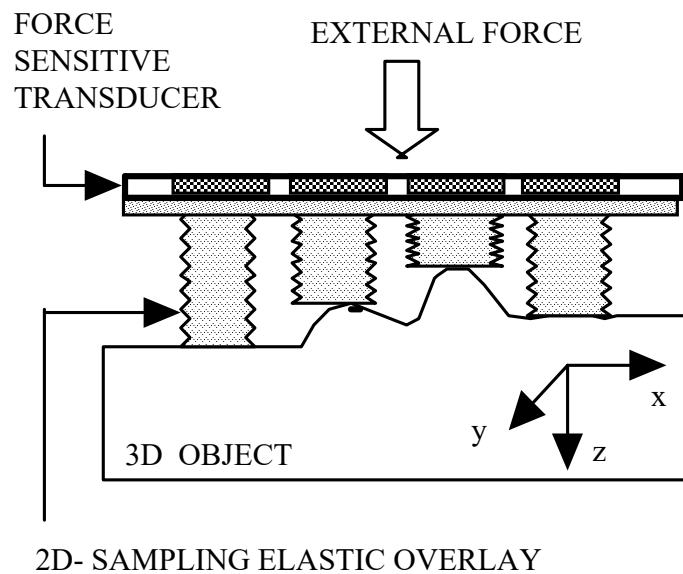
The **elastic overlay** provides a *geometric profile-to-force* transduction function. The resulting forces are the measured by FSR.

[from E.M. Petriu, S.R. Das, S.K. Yeung, "Robotic Tactile Perception," *Proc. IMTC/99, IEEE Instrum. Meas. Technol. Conf.*, pp. 1266-1271, Venice, Italy, May 1999.]



The 16-by-16 matrix of Force Sensing Resistors (FSR), spaced 1.58 mm apart on a 6.5 cm² (1 sq. inch) area. The FSR elements have an exponentially decreasing electrical resistance with applied normal force: the resistance changes by two orders of magnitude over a pressure range of 1 N/cm² to 100 N/cm².

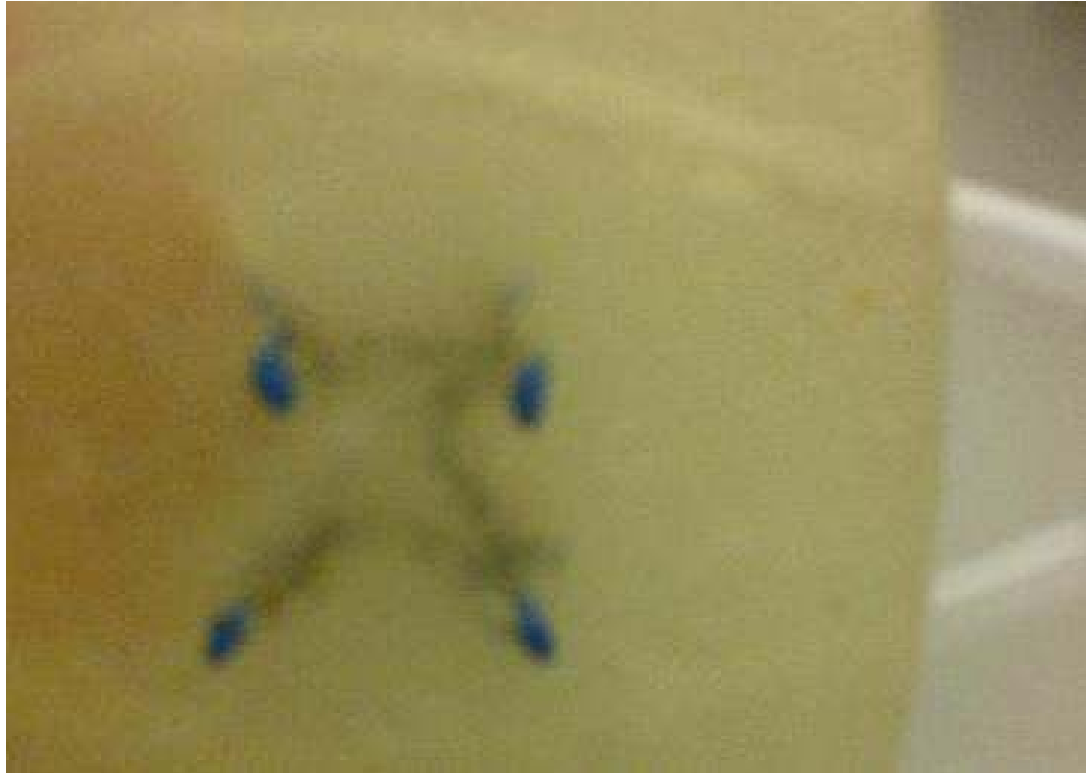




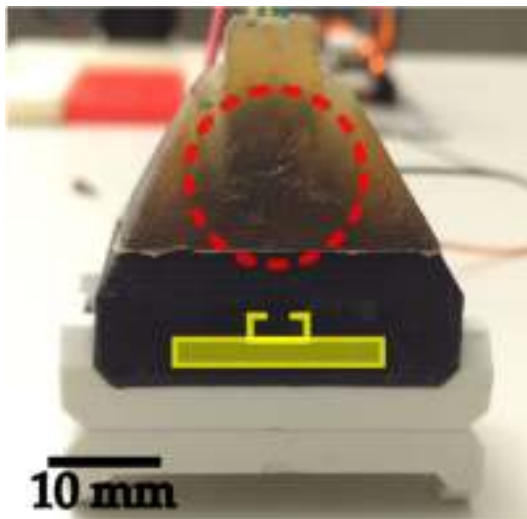
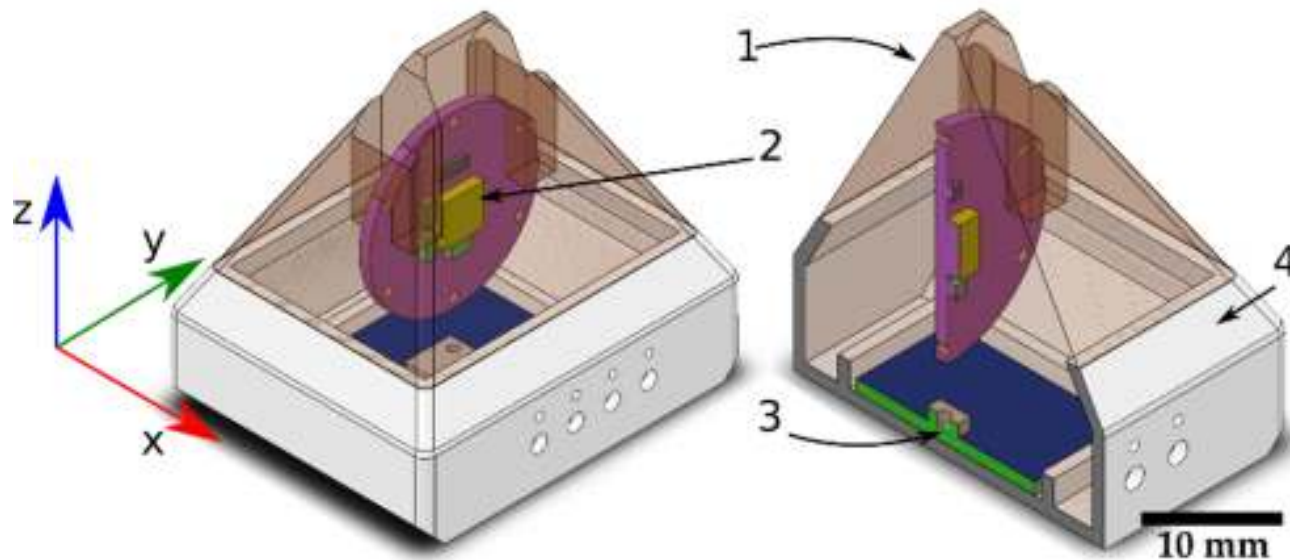
The **elastic overlay** has a protective damping effect against impulsive contact forces and its elasticity resets the probe when it ceases to touch the object.

The crosstalk effect present in one-piece elastic pads produces considerable blurring distortions. It is possible to reduce this by using a **custom-designed elastic overlay consisting of a relatively thin membrane with protruding round tabs**. This construction allows free space for the material to expand in the x and y directions allowing for a compression in the z direction proportional with the stress component along this axis.

[from E.M. Petriu, S.R. Das, S.K. Yeung, "Robotic Tactile Perception," *Proc. IMTC/99, IEEE Instrum. Meas. Technol. Conf.*, pp. 1266-1271, Venice, Italy, May 1999.]



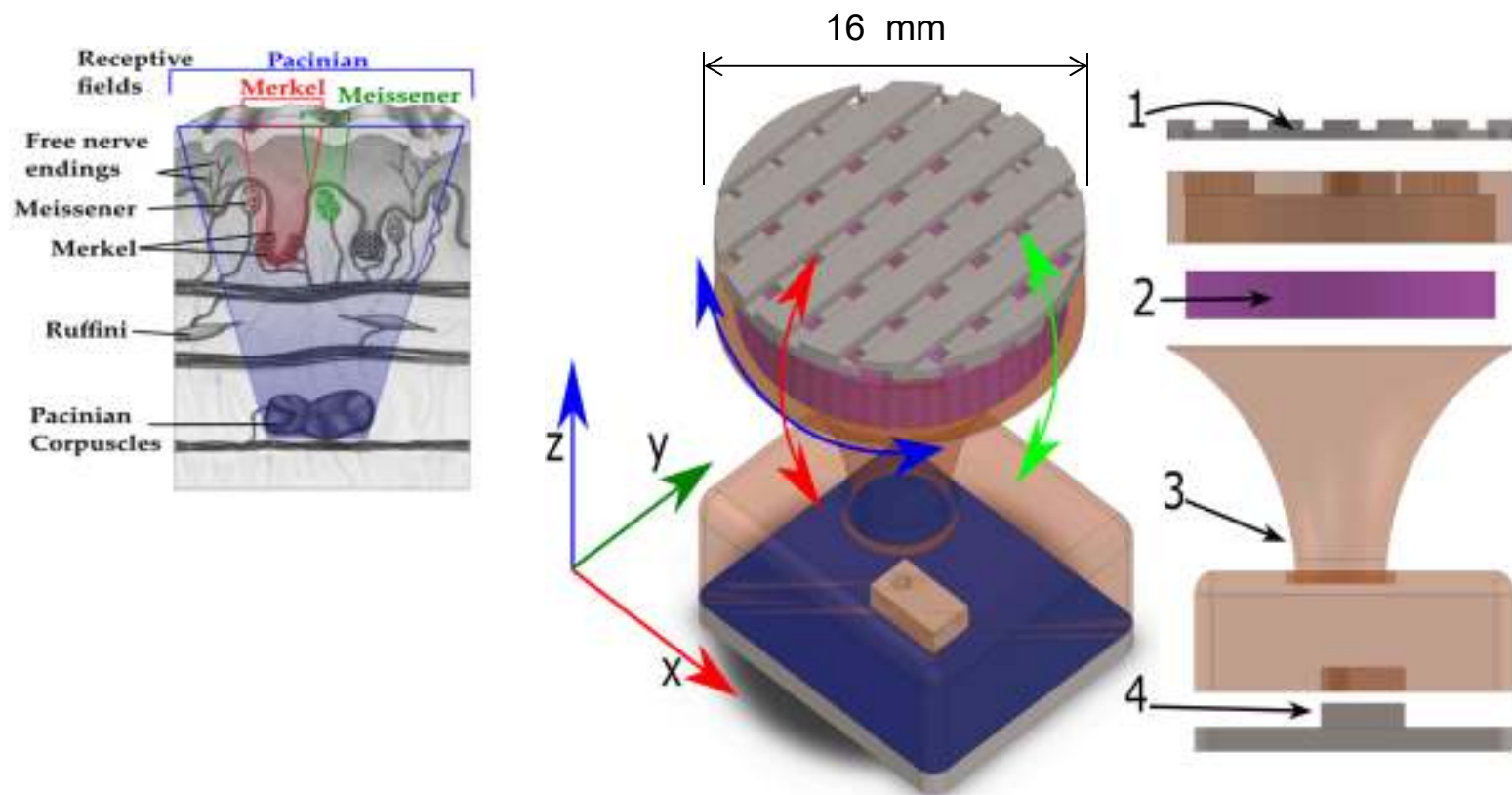
Tactile sensing artificial skin using **Rufini corpuscles -like** thermistors and a **blood-vessel like source of heat** distributed within the elastic skin. [from E.M. Petriu, "Biology-Inspired Multimodal Tactile Sensor System," *Proc. ROSE 2011, IEEE Int. Symp. Robotic and Sensor Environments*, pp. 54-59, Montreal, Que, Canada, Sep. 2011]



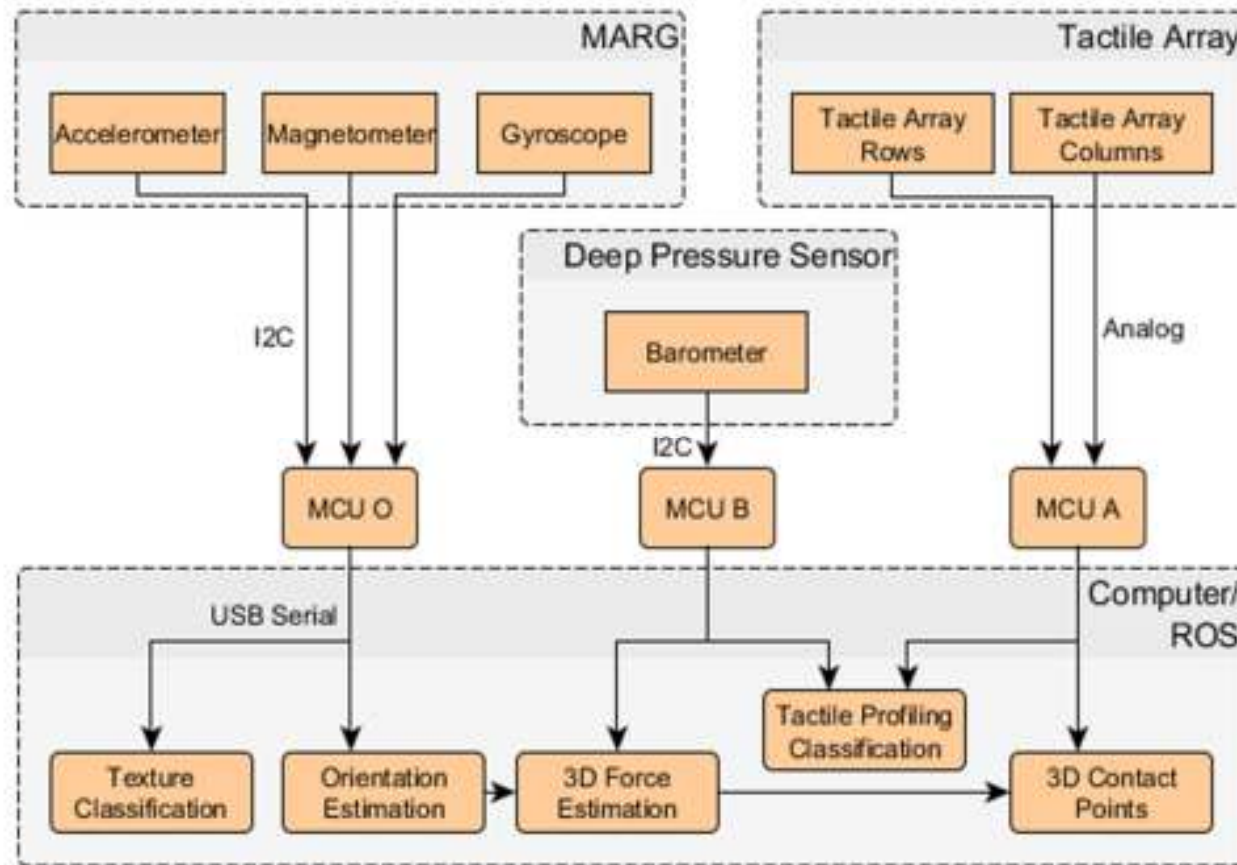
Tactile-enabled fingertip for dynamic exploration of surfaces

(1) Elastic skin; (2) MARG (Magnetic, Angular Rate, and Gravity) sensor measures vibrations, accelerations, angular velocities and changes in the magnetic field emulating the functions of [Merkel cells](#) and [Meissner corpuscles](#); (3) deep pressure sensor (MEMS barometer sensor emulating the functions of [Pacinian corpuscles](#); and (4) supporting collar.

[from T.E. Alves de Oliveira, A.-M. Cretu, E.M. Petriu, "Multimodal Bio-Inspired Tactile Sensing Module for Surface Characterization," Sensors, MDPI, vol. 17, paper # 1187, pp. 1-19, May 2017]



Bio-inspired Multimodal Tactile Sensing Skin Module: (1) **Merkel disk-** and **Meissner corpuscle-**like shape, pressure, local skin deformation, and slippage sensitive tactile array (32 taxels); (2) **Ruffini corpuscle-** like vibration and stretch sensitive MARG sensor; (3) **compliant skin structure**; (4) **Pacinian corpuscle-**like deep pressure sensor; [from T.E. Alves de Oliveira, A.-M. Cretu, E.M. Petriu, "Multimodal Bio-Inspired Tactile Sensing Module," *IEEE Sensors Journal*, Vol. 17, Issue 11, pp. 3231 – 3243, 2017]



System components and examples of applications for the *multimodal tactile sensing skin module* [from T.E. Alves de Oliveira, A.-M. Cretu, E.M. Petriu, "Multimodal Bio-Inspired Tactile Sensing Module," *IEEE Sensors Journal*, Vol. 17, Issue 11, pp. 3231 – 3243, 2017]



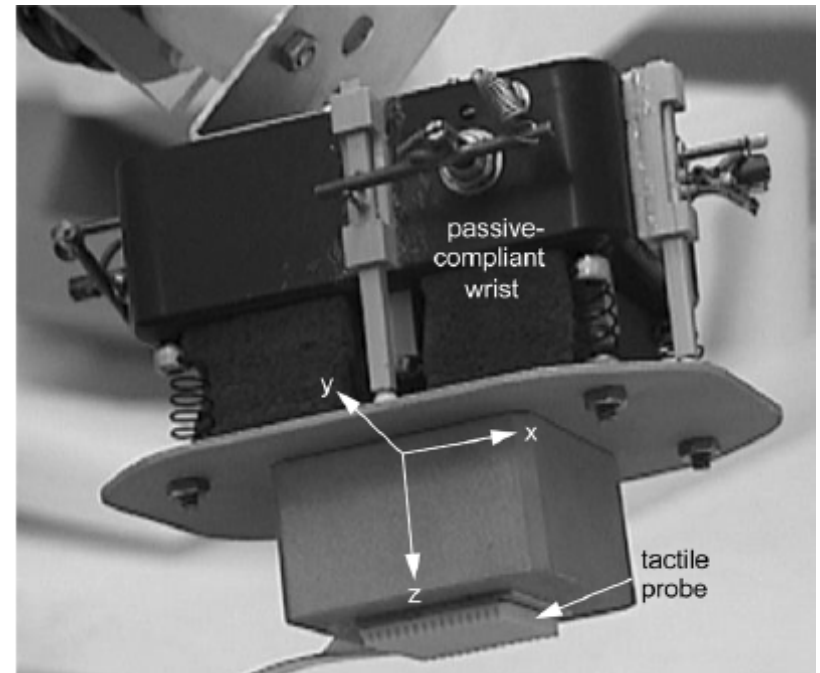
Haptic Perception of Rigid 3D Object Shapes

Haptic perception is the result of an active deliberate contact exploratory sensing act.

A **tactile probe** provides the local “cutaneous” information about the touched area of the object.

A **robotic carrier** providing the “kinesthetic” capability is used to move the tactile probe around on the explored object surface and to provide the contact force needed for the probe to extract the desired cutaneous information (e.g. local 3D geometric shape, elastic properties, and/or termic impedance) of the touched object area .

The local *information provided by the tactile probe is integrated with the kinesthetic position parameters of the carrier* resulting in a composite **haptic model** (global geometric and elastic profiles, termic impedance map) of the explored 3D object.

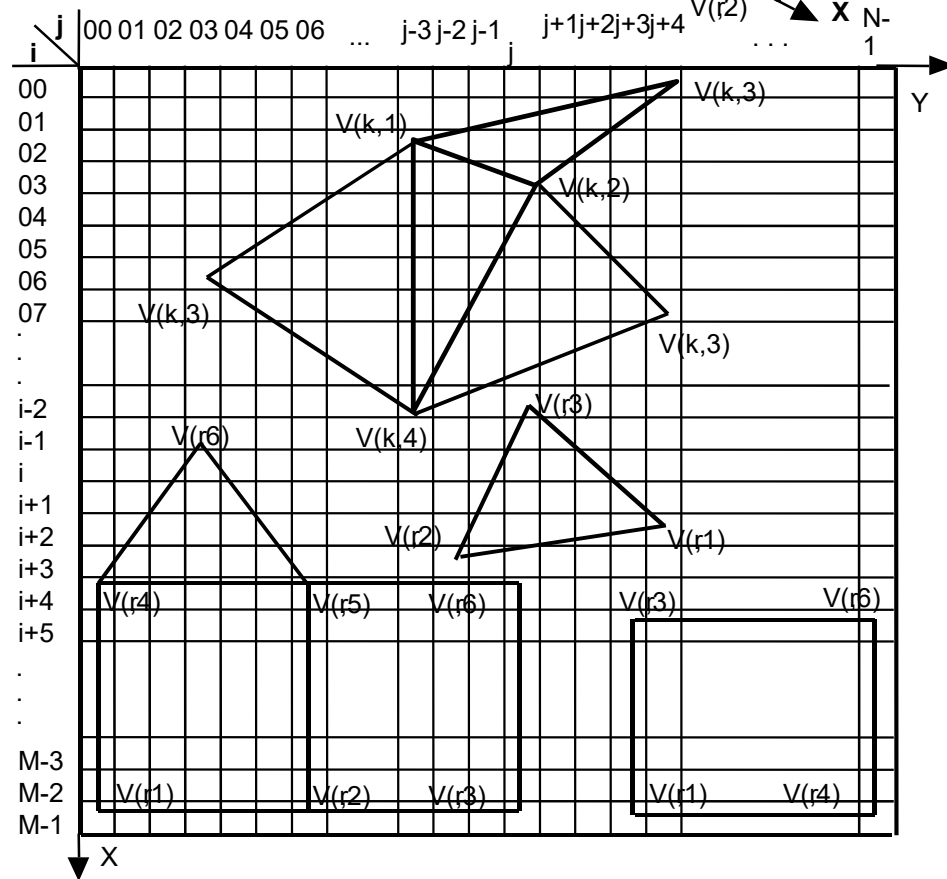
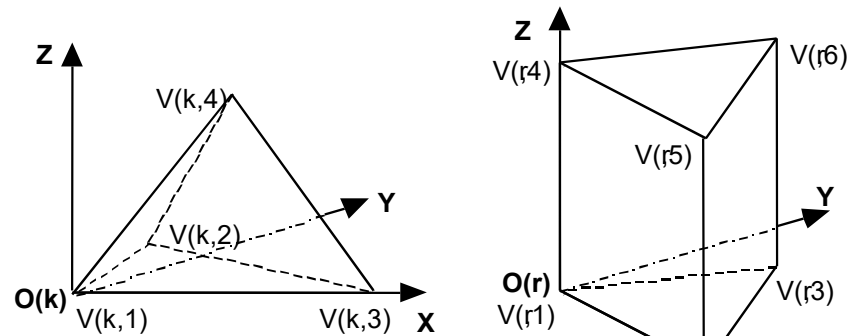


Robotic finger-like articulated structure with instrumented **passive-compliant joint** and a **tactile probe** array. Position sensors placed in the robot joints and on the instrumented passive-compliant wrist provide the kinesthetic information. The compliant wrist allows the probe to accommodate the constraints of the touched object surface and thus to increase the local cutaneous information extracted during the active exploration process under the force provided by the robotic finger,. [from P. Payeur, C. Pasca, A.-M. Cretu, E.M. Petriu, "Intelligent Haptic Sensor System for Robotic Manipulation," *IEEE Tr. Instrum. Meas.*, Vol. 54, No. 4, pp. 1583 – 1592, 2005.]

Model-based tactile object recognition

PRA code elements are Braille-like embossed on object surfaces: 3D object models are unfolded and mapped on the encoding pseudo-random array.

[from E.M. Petriu, S.K.S. Yeung, S.R. Das, A.M. Cretu, H.J.W. Spoelder, "Robotic Tactile Recognition of Pseudorandom Encoded Objects, IEEE Trans. Instrum. Meas., Vol.53, No.5, pp.1425-1432, 2004.]



0	A	1	A ²	A	A ²	A ²	A ²	1	1	A ²	A ²	A ²	A	A ²	1	A
0	0	1	A ²	A ²	A	1	0	A ²	A ²	0	1	A	A ²	A ²	1	0
0	A ²	0	0	A	A	A ²	1	A ²	A ²	1	A ²	A	A	0	0	A ²
0	1	A	1	A	0	A ²	A	0	0	A	A ²	0	A	1	A	1
0	A ²	A ²	A	0	A ²	0	1	1	1	1	0	A ²	0	A	A ²	A ²
0	A ²	A	1	A ²	1	1	1	A	A	1	1	1	A ²	1	A	A ²
0	0	A	1	1	A ²	A	0	1	1	0	A	A ²	1	1	A	0
0	1	0	0	A ²	A ²	1	A	1	1	A	1	A ²	A ²	0	0	1
0	A	A ²	A	A ²	0	1	A ²	0	0	A ²	1	0	A ²	A	A ²	A
0	1	1	A ²	0	1	0	A	A	A	A	0	1	0	A ²	1	1
0	1	A ²	A	1	A	A	A	A ²	A ²	A	A	A	1	A	A ²	1
0	0	A ²	A	A	1	A ²	0	A	A	0	A ²	1	A	A	A ²	0
0	A	0	0	1	1	A	A ²	A	A	A ²	A	1	1	0	0	A
0	A ²	1	A ²	1	0	A	1	0	0	1	A	0	1	A ²	1	A ²
0	A	A	1	0	A	0	A ²	A ²	A ²	A ²	0	A	0	1	A	A

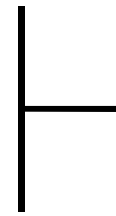
15-by-17 PRA obtained by folding a 255 element PRS defined over GF(4), with $q=4$, $n=4$, $k_1=2$, $k_2=2$, $n_1=q^{k_1}-1=15$, and $n_2=(q^n-1)/n_1=17$

The shape of the embossed symbols is specially designed for easy tactile recognition. For an efficient pattern recognition, the particular shape of the binary symbols were selected in such a way to meet the following conditions:

- (i) there is enough information at the symbol level to provide an immediate indication of the grid orientation;
- (ii) the symbol recognition procedure is invariant to position, and orientation;
- (iii) the symbols have a certain peculiarity so that other objects in the scene will not be mistaken for encoding symbols.

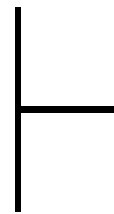


“0”



“1”

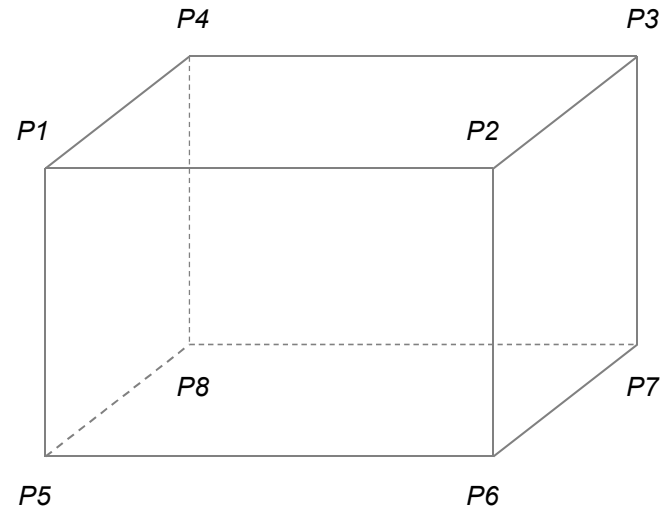
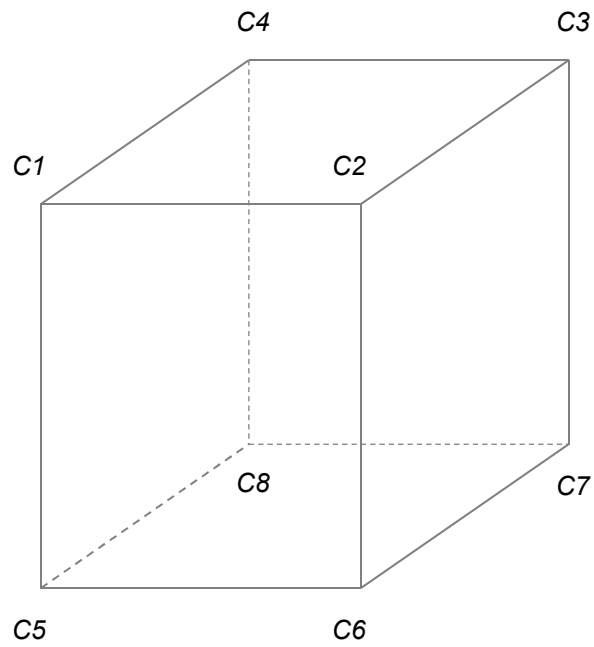
The shape of the four code symbols for a PRA over $GF(4)$ embossed on object's surface



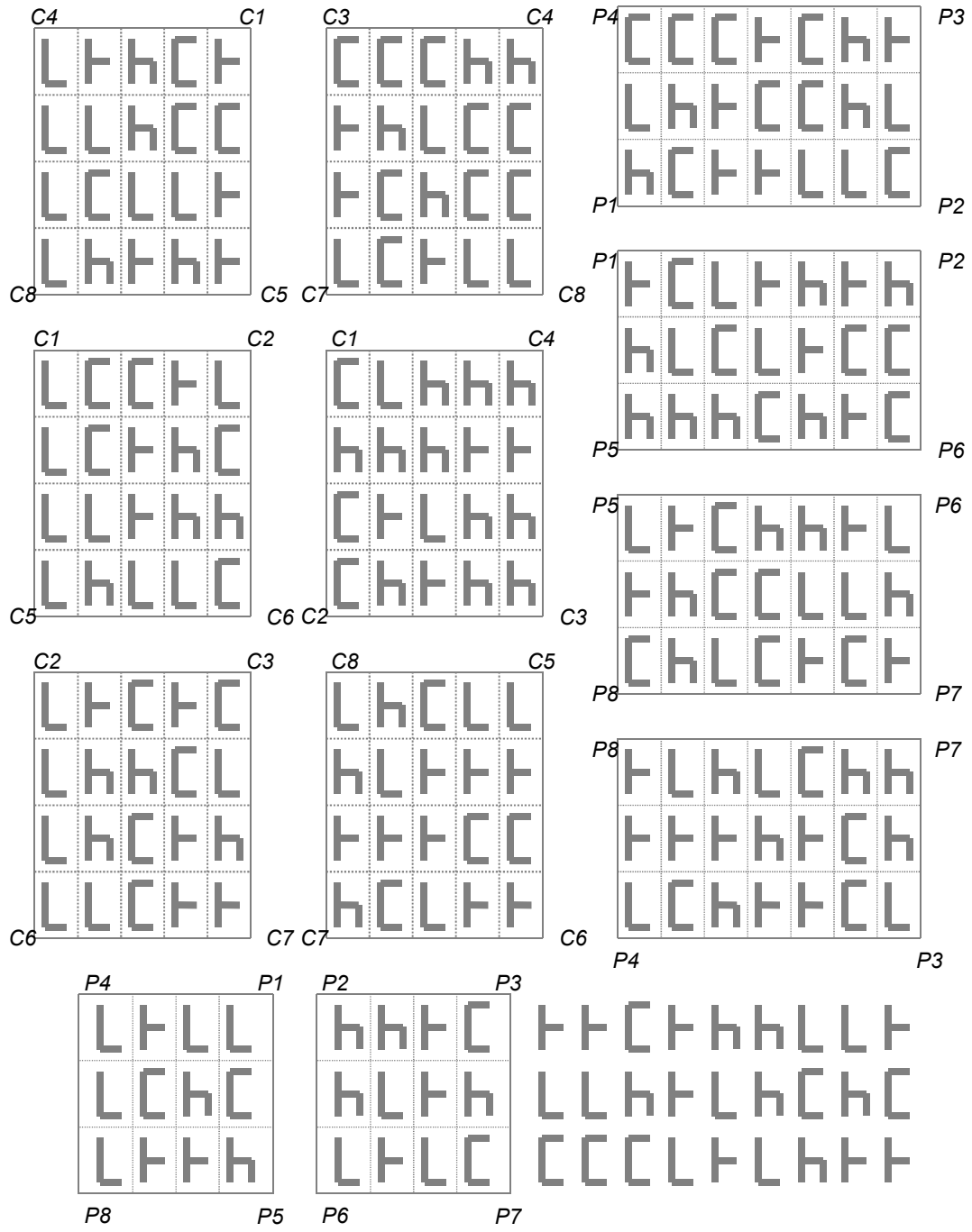
“A”



“A²”



The vertex labeled models of two simple 3D objects



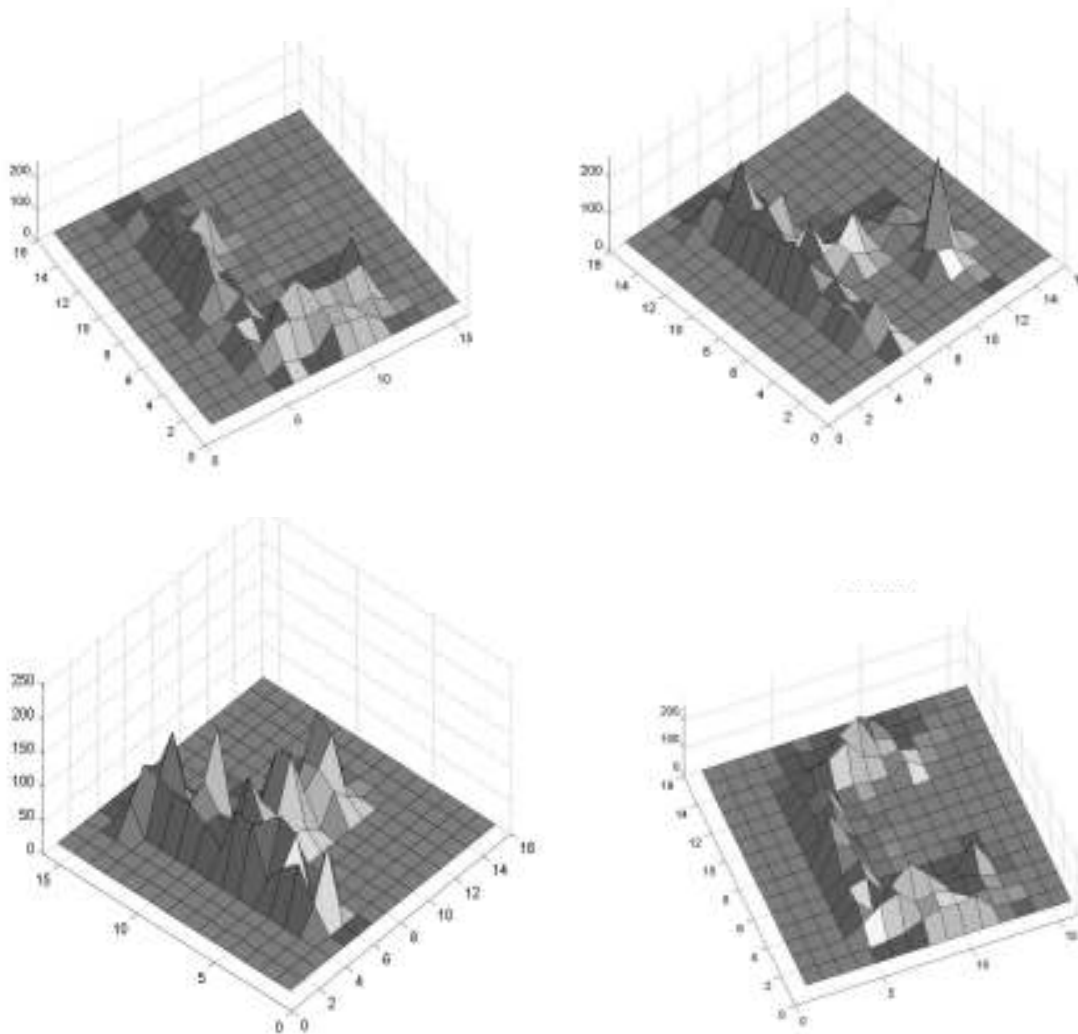
Mapping the embossed PRBA on the surfaces of the two 3D objects

[from E.M. Petriu, S.K.S. Yeung, S.R. Das, A.M. Cretu, H.J.W. Spoelder, "Robotic Tactile Recognition of Pseudorandom Encoded Objects, IEEE Trans. Instrum. Meas., Vol.53, No.5, pp.1425-1432, 2004.)]



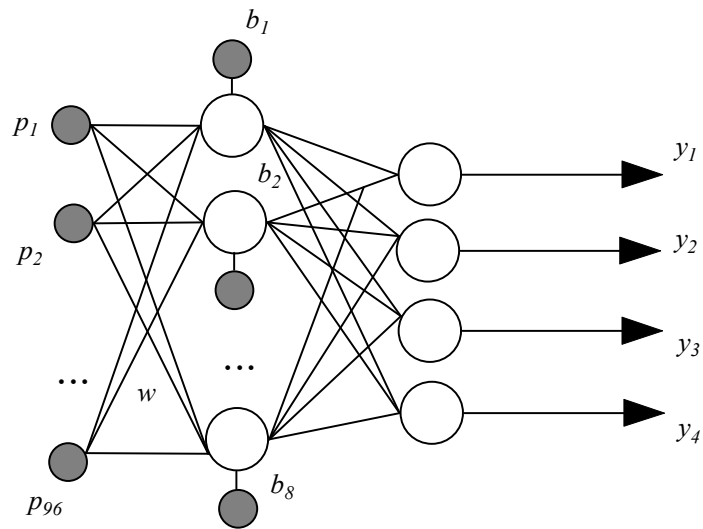
The PRA encoded cube.

[from E.M. Petriu, S.K.S. Yeung, S.R. Das, A.M. Cretu, H.J.W. Spoelder, "Robotic Tactile Recognition of Pseudorandom Encoded Objects, IEEE Trans. Instrum. Meas., Vol.53, No.5, pp.1425-1432, 2004.]

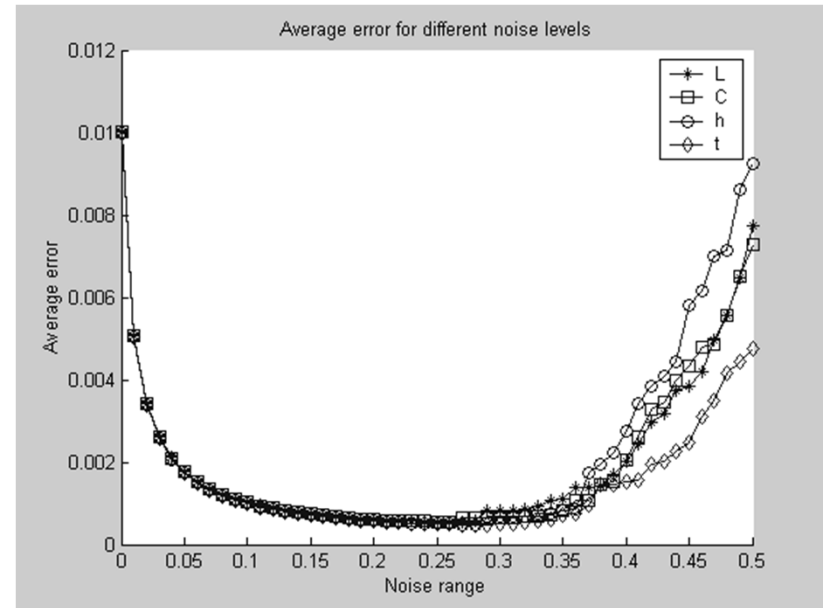


Tactile images of the four GF(4) symbols. The two rectangular axes on the horizontal plane in each image indicate the 2D node coordinates of the 16-by-16 tactile image. One unit on the vertical axis corresponds to 0.015875 mm (0.01/16 inch).

[from E.M. Petriu, S.K.S. Yeung, S.R. Das, A.M. Cretu, H.J.W. Spoelder, "Robotic Tactile Recognition of Pseudorandom Encoded Objects, IEEE Trans. Instrum. Meas., Vol.53, No.5, pp.1425-1432, 2004.)]

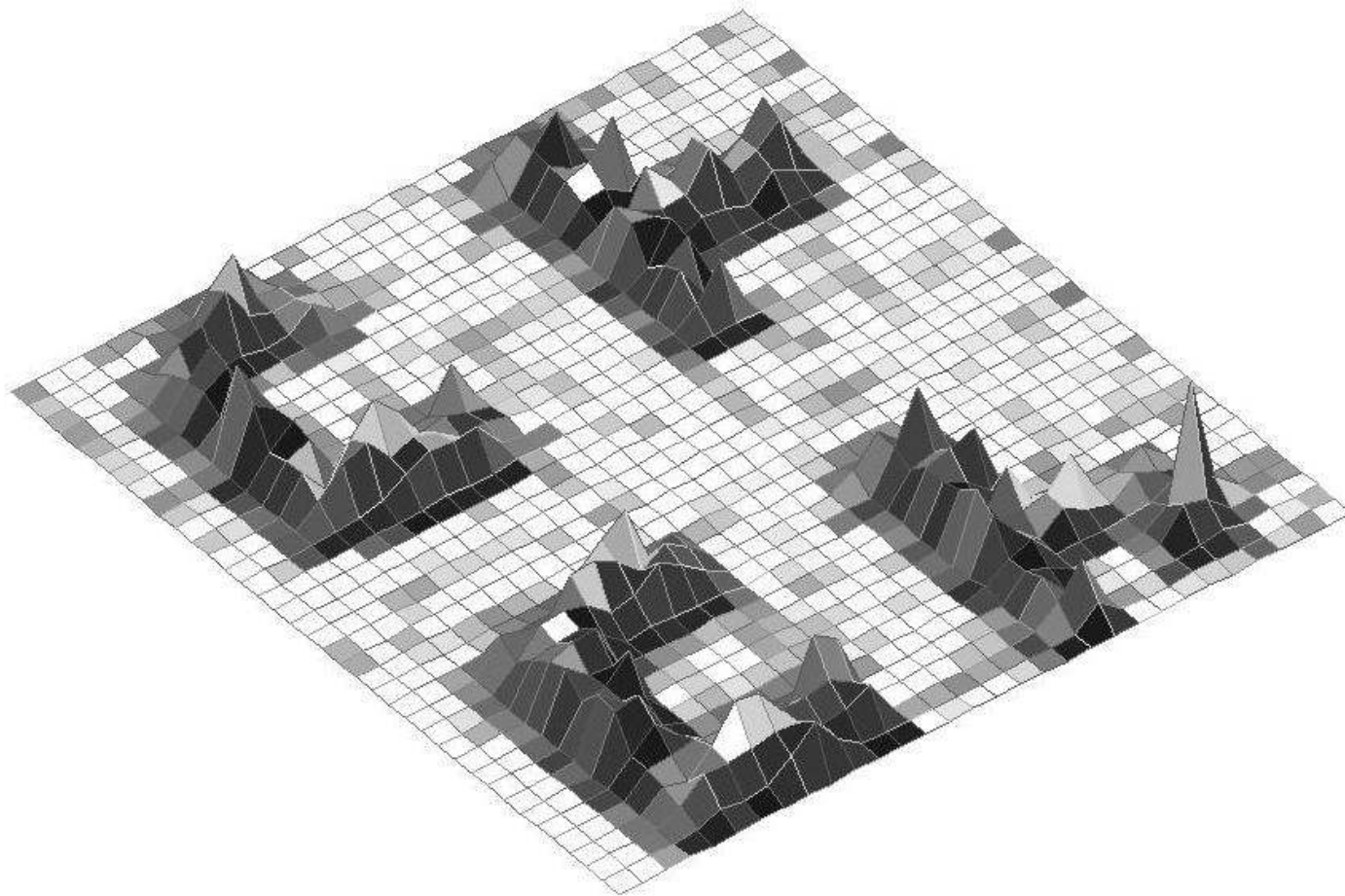


Two-layer feed-forward NN architecture for the classification of the four GF(4) symbols.



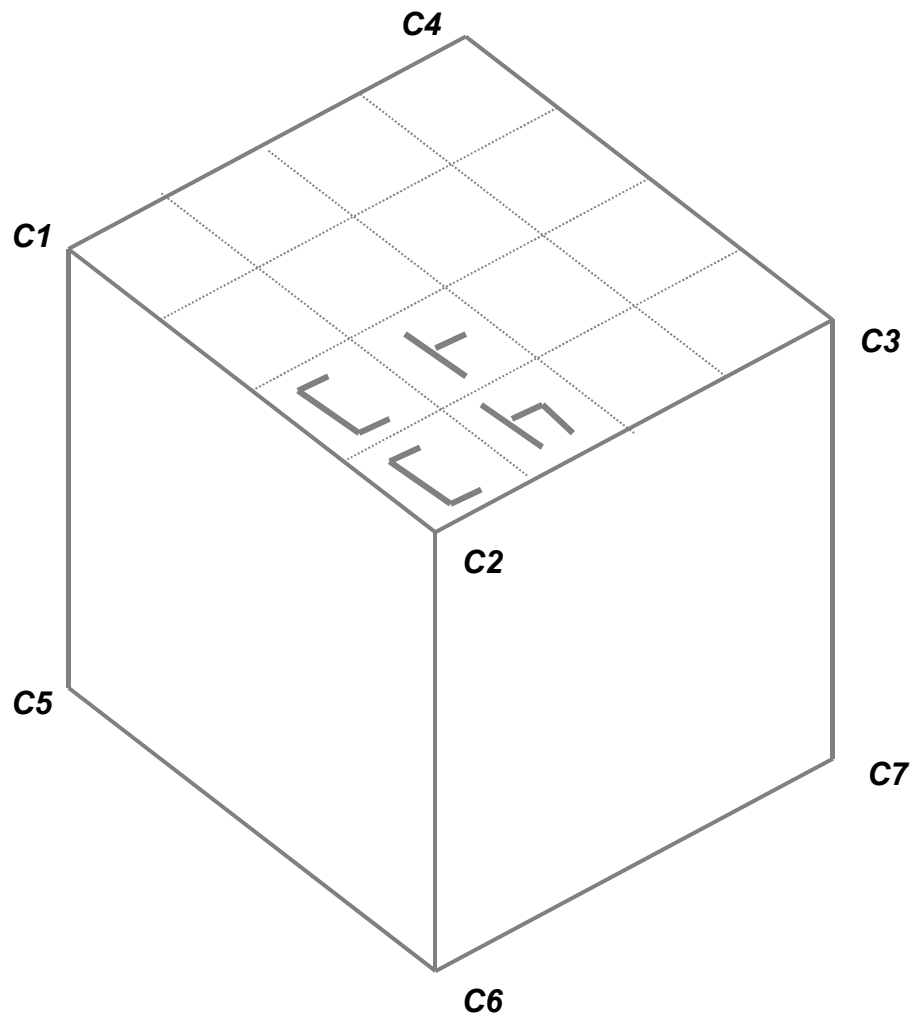
Average error rate for noise ranging between 0 and 0.5

[from E.M. Petriu, S.K.S. Yeung, S.R. Das, A.M. Cretu, H.J.W. Spoelder, "Robotic Tactile Recognition of Pseudorandom Encoded Objects, IEEE Trans. Instrum. Meas., Vol.53, No.5, pp.1425-1432, 2004.]



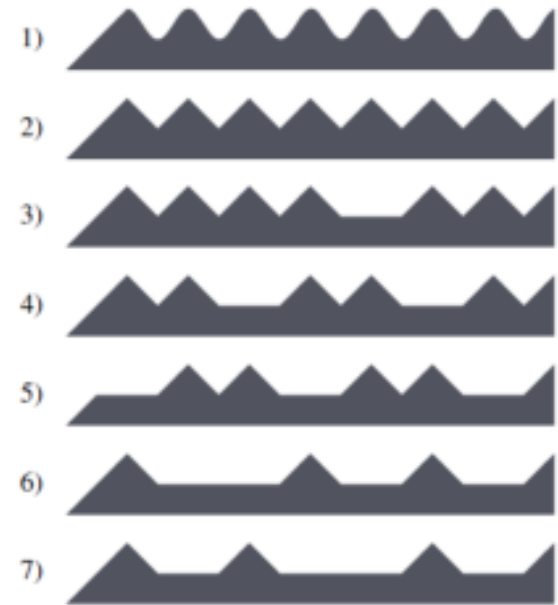
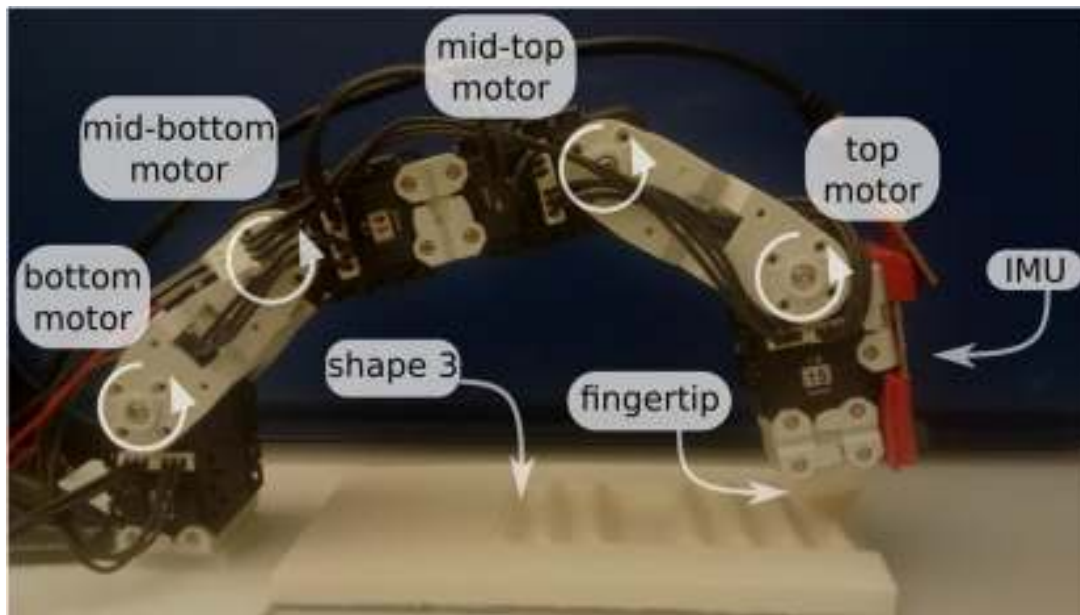
Composite tactile image of four symbols
on an encoded object surface

[from E.M. Petriu, S.K.S. Yeung, S.R. Das, A.M. Cretu, H.J.W. Spoelder, "Robotic Tactile Recognition of Pseudorandom Encoded Objects, IEEE Trans. Instrum. Meas., Vol.53, No.5, pp.1425-1432, 2004.)]



The four tactile recovered symbols are recognized, And their location is unequivocally identified on the face of one of the 3D objects, using the PRA window property.

[from E.M. Petriu, S.K.S. Yeung, S.R. Das, A.M. Cretu, H.J.W. Spoelder, "Robotic Tactile Recognition of Pseudorandom Encoded Objects, IEEE Trans. Instrum. Meas., Vol.53, No.5, pp.1425-1432, 2004.)]



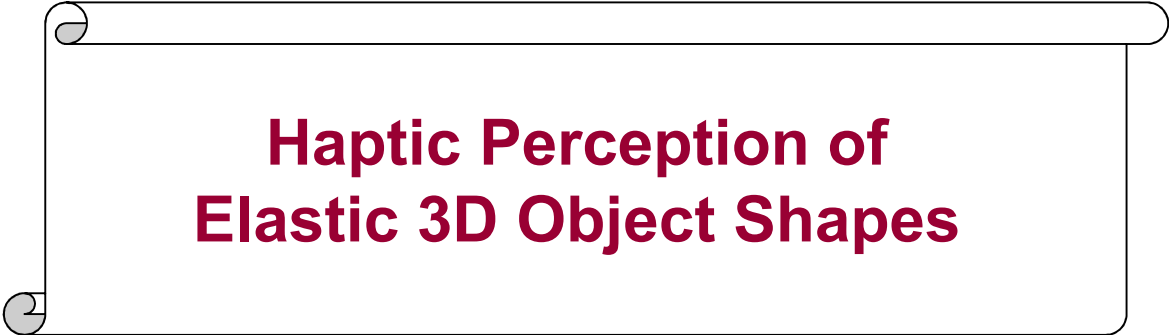
Tactile-enabled fingertip exploring various texture profiles

[from T.E. Alves de Oliveira, A.-M. Cretu, E.M. Petriu, "Multimodal Bio-Inspired Tactile Sensing Module for Surface Characterization," *Sensors*, MDPI, vol. 17, paper # 1187, pp. 1-19, May 2017].

Output Class	1	25 14.3%	0 0.0%	0 0.0%	0 0.0%	0 0.0%	0 0.0%	0 0.0%	100%
	2	0 0.0%	25 14.3%	0 0.0%	0 0.0%	0 0.0%	0 0.0%	0 0.0%	100%
	3	0 0.0%	0 0.0%	25 14.3%	0 0.0%	0 0.0%	0 0.0%	0 0.0%	100%
	4	0 0.0%	0 0.0%	0 0.0%	25 14.3%	2 1.1%	0 0.0%	0 0.0%	92.6%
	5	0 0.0%	0 0.0%	0 0.0%	0 0.0%	23 13.1%	0 0.0%	0 0.0%	100%
	6	0 0.0%	0 0.0%	0 0.0%	0 0.0%	0 0.0%	25 14.3%	0 0.0%	100%
	7	0 0.0%	0 0.0%	0 0.0%	0 0.0%	0 0.0%	0 0.0%	25 14.3%	100%
			100%	100%	100%	100%	92.0%	100%	100%
		0.0%	0.0%	0.0%	0.0%	8.0%	0.0%	0.0%	1.1%
		1	2	3	4	5	6	7	
		Target Class							

Output Class	1	23 13.1%	8 4.6%	6 3.4%	3 1.7%	0 0.0%	0 0.0%	0 0.0%	57.5%
	2	2 1.1%	17 9.7%	1 0.6%	0 0.0%	0 0.0%	1 0.6%	0 0.0%	81.0%
	3	0 0.0%	0 0.0%	18 10.3%	0 0.0%	0 0.0%	1 0.6%	0 0.0%	94.7%
	4	0 0.0%	0 0.0%	0 0.0%	21 12.0%	0 0.0%	2 1.1%	0 0.0%	91.3%
	5	0 0.0%	0 0.0%	0 0.0%	0 0.0%	25 14.3%	0 0.0%	1 0.6%	96.2%
	6	0 0.0%	0 0.0%	0 0.0%	1 0.6%	0 0.0%	21 12.0%	0 0.0%	95.5%
	7	0 0.0%	0 0.0%	0 0.0%	0 0.0%	0 0.0%	0 0.0%	24 13.7%	100%
			92.0%	88.0%	72.0%	84.0%	100%	84.0%	96.0%
		8.0%	32.0%	28.0%	16.0%	0.0%	16.0%	4.0%	14.9%
		1	2	3	4	5	6	7	
		Target Class							

Confusion tables for: (left) barometer, showing the misclassification of Shape 5 as Shape 4; and (right) accelerometer on x-axis, showing the misclassification between Shapes 1 and 2 [from T.E. Alves de Oliveira, A.-M. Cretu, E.M. Petriu, "Multimodal Bio-Inspired Tactile Sensing Module for Surface Characterization," *Sensors*, MDPI, vol. 17, paper # 1187, pp. 1-19, May 2017].



**Haptic Perception of
Elastic 3D Object Shapes**

- ❑ **“Improved accuracy and richness in object modeling and haptic rendering** will require advances in our understanding of how to represent and render psychophysically and cognitively germane attributes of objects, as well as algorithms and perhaps specialty hardware (such as ***haptic or physics engines***) to perform real-time computations” [K. Salisbury, F. Conti, F. Barbagli, “Haptic Rendering: Introductory Concepts,” *IEEE Computer Graphics and Applications*, Vol. 24, No. 2, pp. 24 – 32, 2004].

- ❑ **Neural Networks** which are able to learn nonlinear behaviors from a limited set of measurement data can **provide efficient and compact multi-media object modeling solutions**. Due to their continuous, analog-like, memory behavior, NNs are able to provide instantaneously an estimation of the output value for input values that were not part of the initial training set.

- ❑ **NNs** consisting of a collection of simple neuron circuits provide **the massive computational parallelism offering efficient storage, model transformation, and real-time rendering capabilities for large numbers of composite geometric & haptic object models** involved in the model-based interactive telemanipulation.

Recovery of the elastic material properties requires touching each point of interest on the explored object surface and then conducting a strain-stress relation measurement on each point.

Tactile probing is a time consuming Sequential operation



Find fast sampling procedures able to minimize the number of the sampling points by selecting only those points that are relevant to the elastic characteristics.



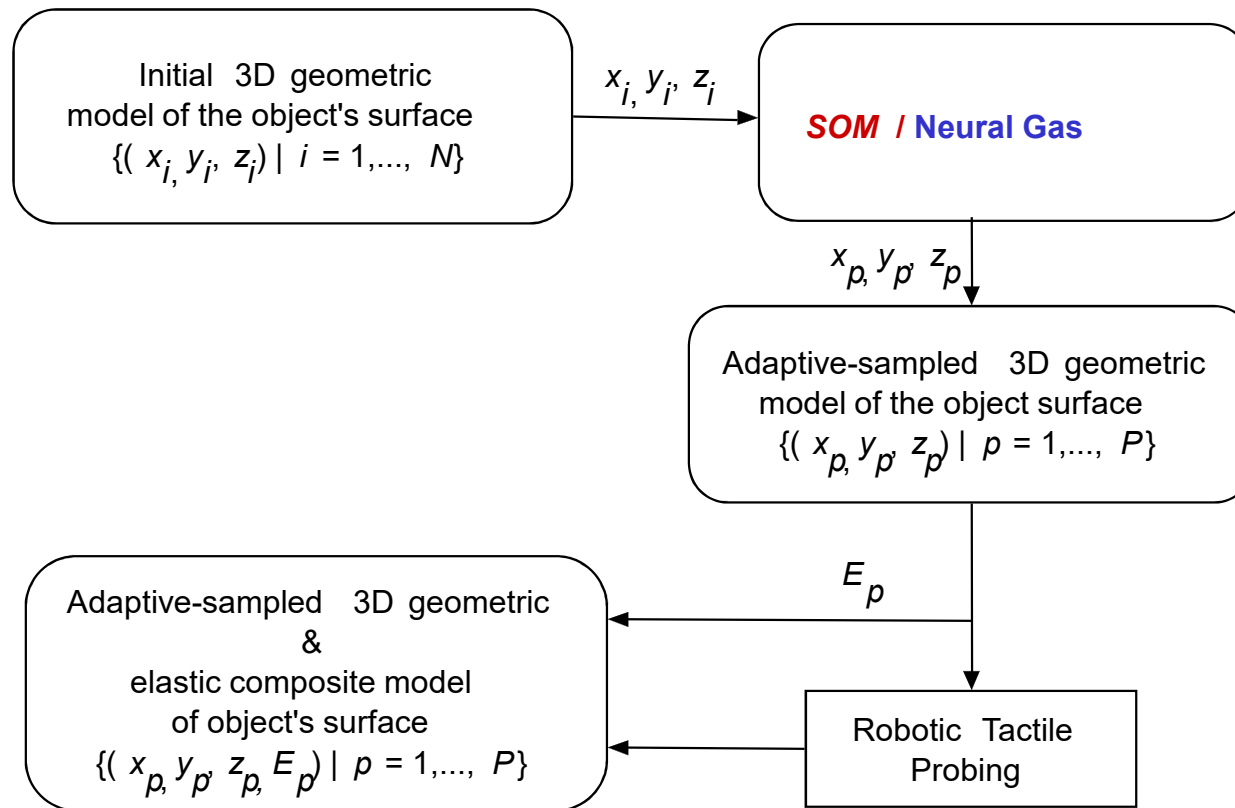
non-uniform adaptive sampling algorithm of the object's surface, which exploits the SOM (self-organizing map) ability to find optimal finite quantization of the input space.

The elastic behaviour at any given point (x_p, y_p, z_p) on the object surface is described by the Hooke's law:

$$\begin{cases} \sigma_p = E_p \cdot \varepsilon_p & \text{if } 0 \leq \varepsilon_p \leq \varepsilon_{p \max} \\ \sigma_p = \sigma_{p \max} & \text{if } \varepsilon_{p \max} < \varepsilon_p \end{cases}$$

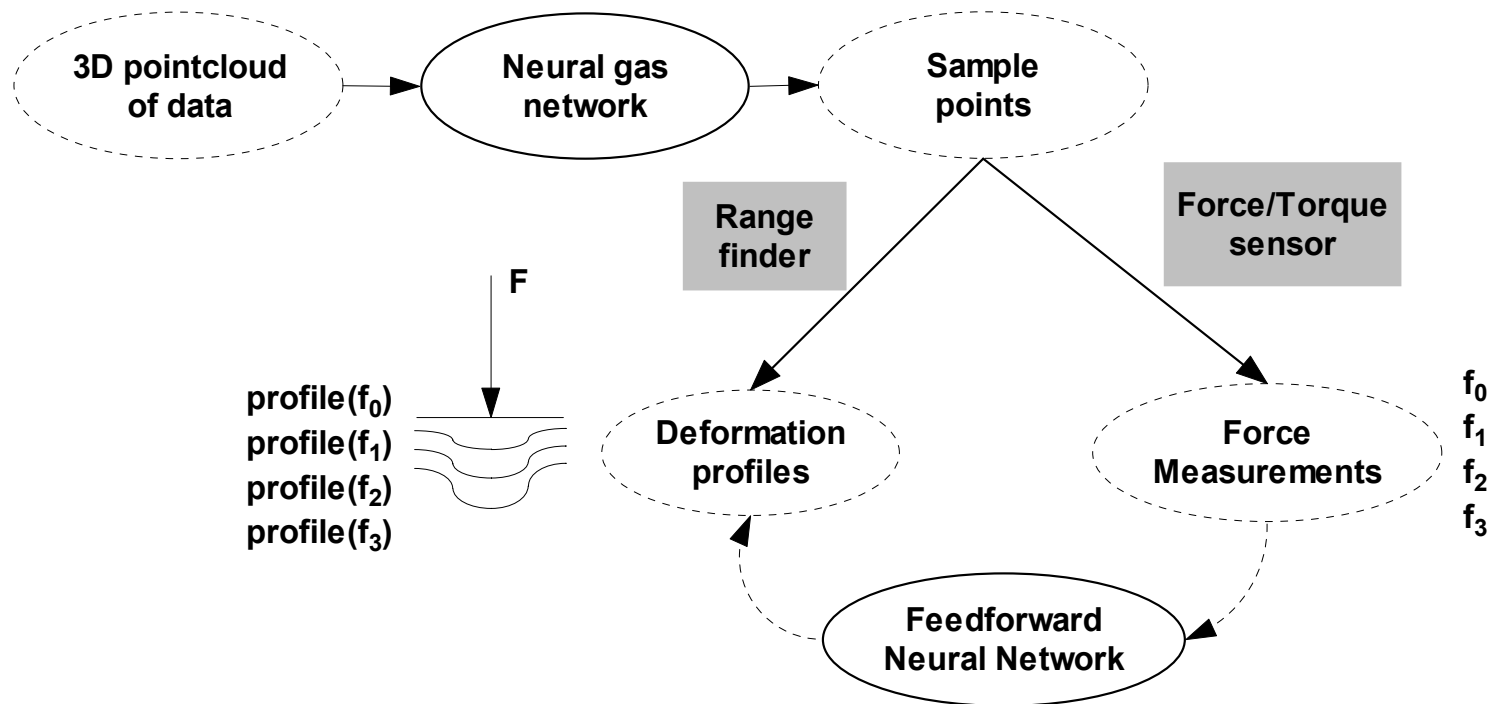
where E_p is the modulus of elasticity , s_p is the stress, and e_p is the strain on the normal direction.

Adaptive Sampling Control of of Elastic Properties of 3D Object Surfaces



[from A.-M. Cretu, E.M. Petriu, "Neural-Network –Based Adaptive Sampling of Three-Dimensional-Object Surface Elastic Properties," *IEEE Trans. Instrum. Meas.*, "Vol. 55, No. 2, pp. 483-492, 2006.]

Neural Network Mapping an Clustering of Elastic Behavior from Tactile and Range Imaging



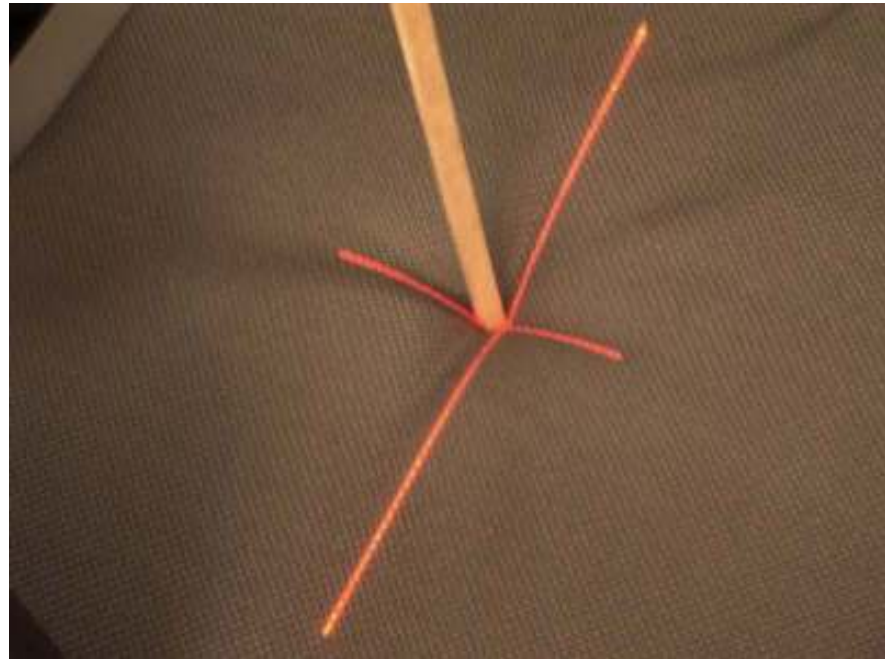
Starting from a 3D point-cloud, a **neural gas NN** yields a reduced set of points that are relevant for further tactile probing. The density of these points is higher in the regions with more pronounced variations in the geometric shape. A **feed-forward NN** is then employed to model the force/displacement behavior of the selected sampling points that are probed simultaneously by a force/torque sensor and an active range finder.

[from A.-M. Cretu, E.M. Petriu, "Neural-Network –Based Adaptive Sampling of Three-Dimensional-Object Surface Elastic Properties," *IEEE Trans. Instrum. Meas.*," Vol. 55, No. 2, pp. 483-492, 2006.]

Recovery of the elastic material properties requires touching each point of interest on the explored object surface and then conducting a strain-stress relation measurement on each point.



Force-torque sensor measuring the interaction force and torque at the point of contact between the robotic probe and the object.

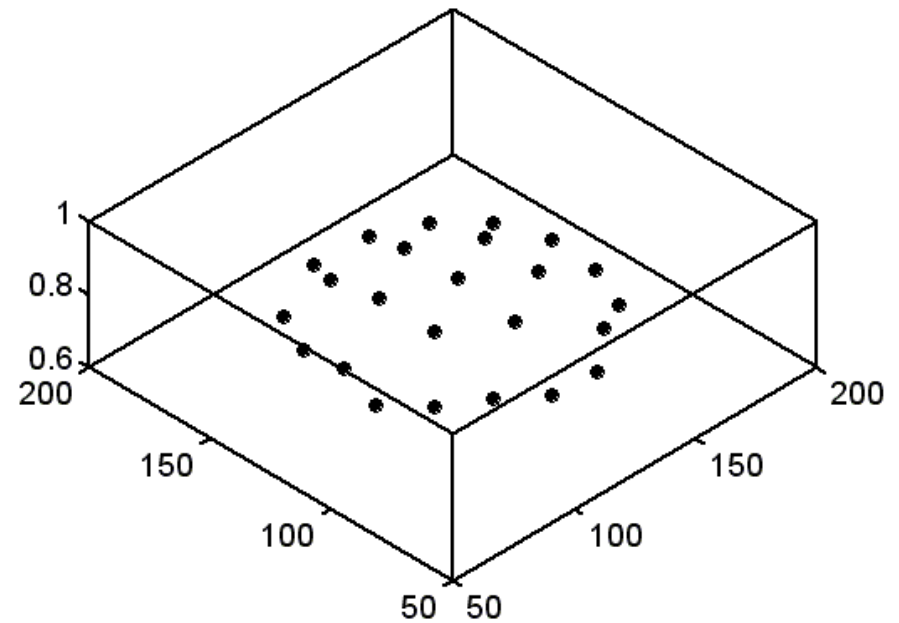


Laser range-finder based recovery of the geometric profiles in an area around the contact point between the probe and the object.

[from A.-M. Cretu, E.M. Petriu, "Neural-Network –Based Adaptive Sampling of Three-Dimensional-Object Surface Elastic Properties," *IEEE Trans. Instrum. Meas.*," Vol. 55, No. 2, pp. 483-492, 2006.]

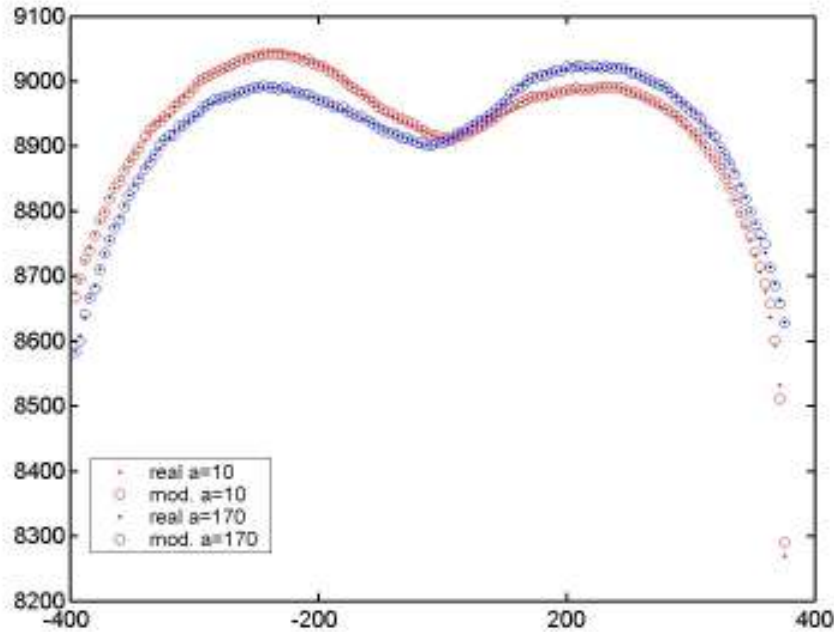


Elastic ball used
for experimentation.

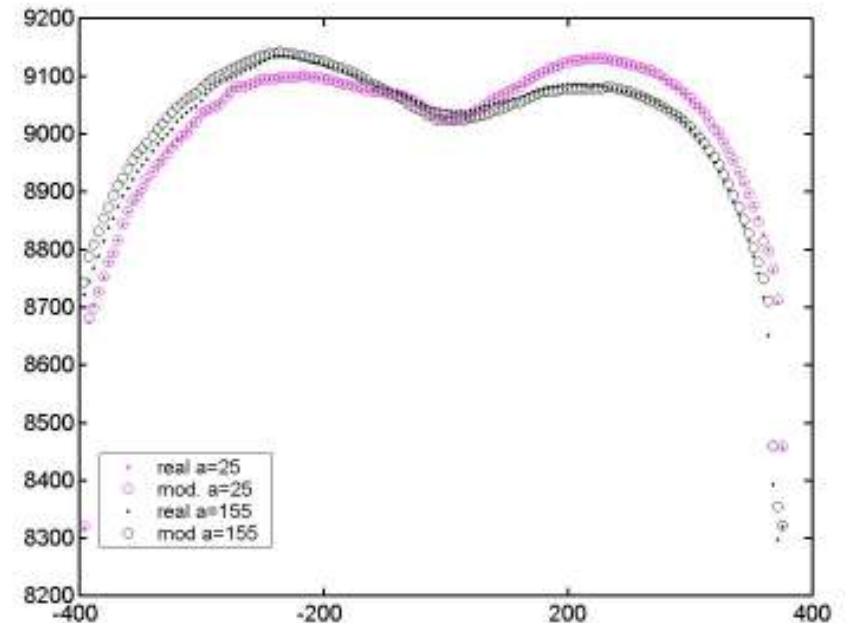


Sampling points selected with
the neural gas network for the ball.

[from A.M. Cretu, E.M. Petriu, P. Payeur "Neural Network Mapping and Clustering of Elastic Behavior from Tactile and Range Imaging for Virtualized Reality Applications," *IEEE Tr. Instr. Meas.*, vol. 57, no. 9, pp. 1918 – 1928, 2008.]



(a)



(b)

Real and **NN modeled** deformation curves using for rubber under forces applied at different angles:

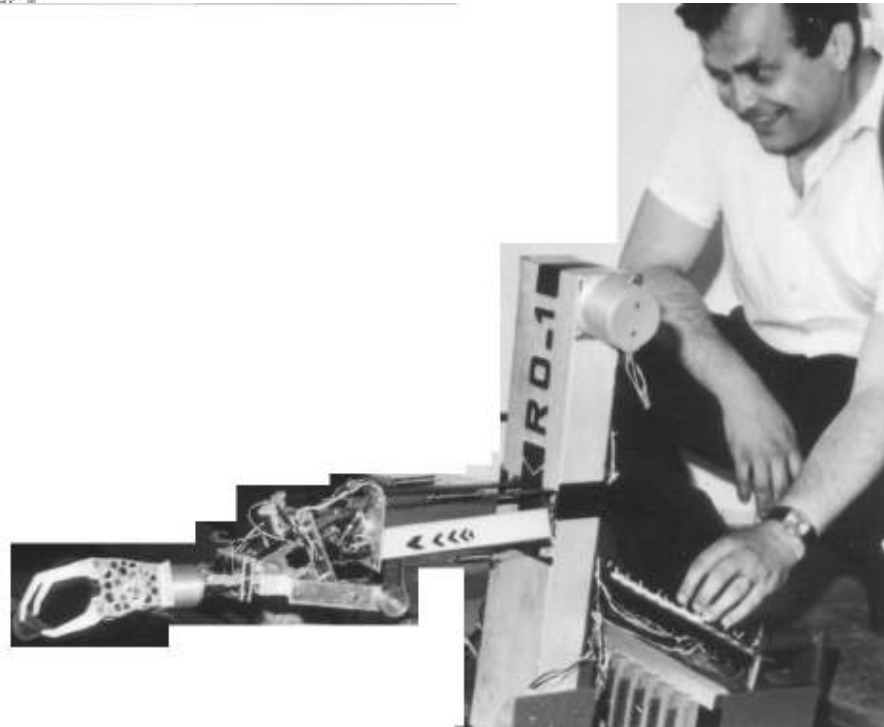
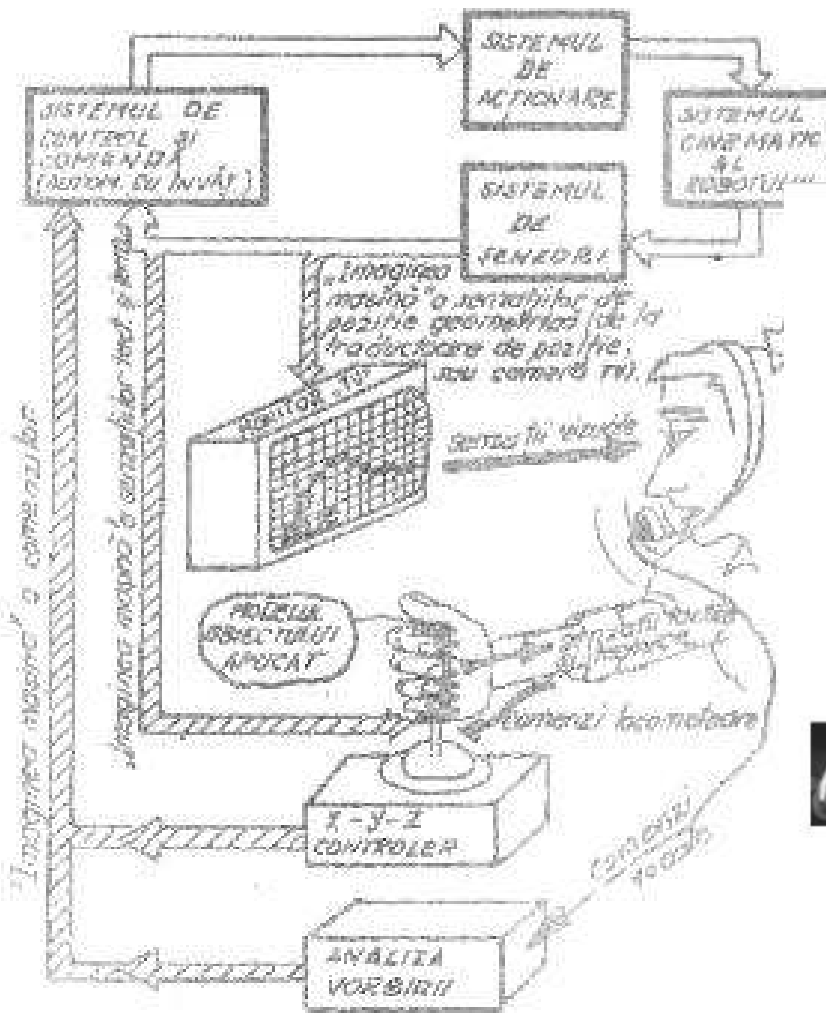
- a) $F=65\text{N}$, $\alpha_1=10^\circ$ and $F=65\text{N}$, $\alpha_2=170^\circ$,
- b) $F=36\text{N}$, $\alpha_1=25^\circ$, and $F=36\text{N}$, $\alpha_2=155^\circ$

[from A.M. Cretu, E.M. Petriu, P. Payeur "Neural Network Mapping and Clustering of Elastic Behavior from Tactile and Range Imaging for Virtualized Reality Applications," *IEEE Tr. Instr. Meas.*, vol. 57, no. 9, pp. 1918 – 1928, 2008.]

Haptic Human-Robot Interfaces

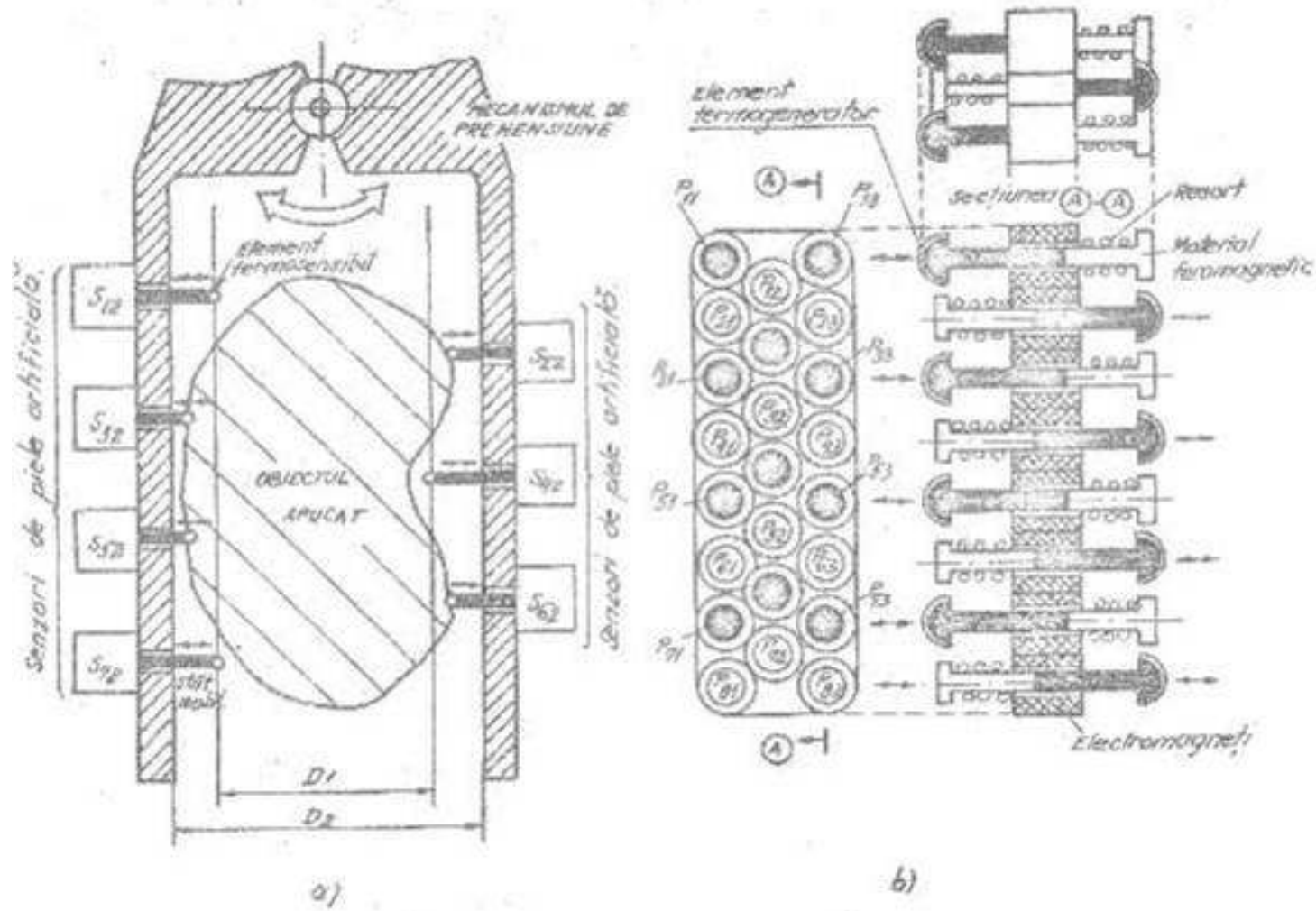
The *haptic human-robot interfaces* should have a bilateral architecture allowing to connect the *human operator* and the *robotic manipulator* as transparently as possible.

Conformal (1:1) mapping of human & robot sensory and perception frameworks

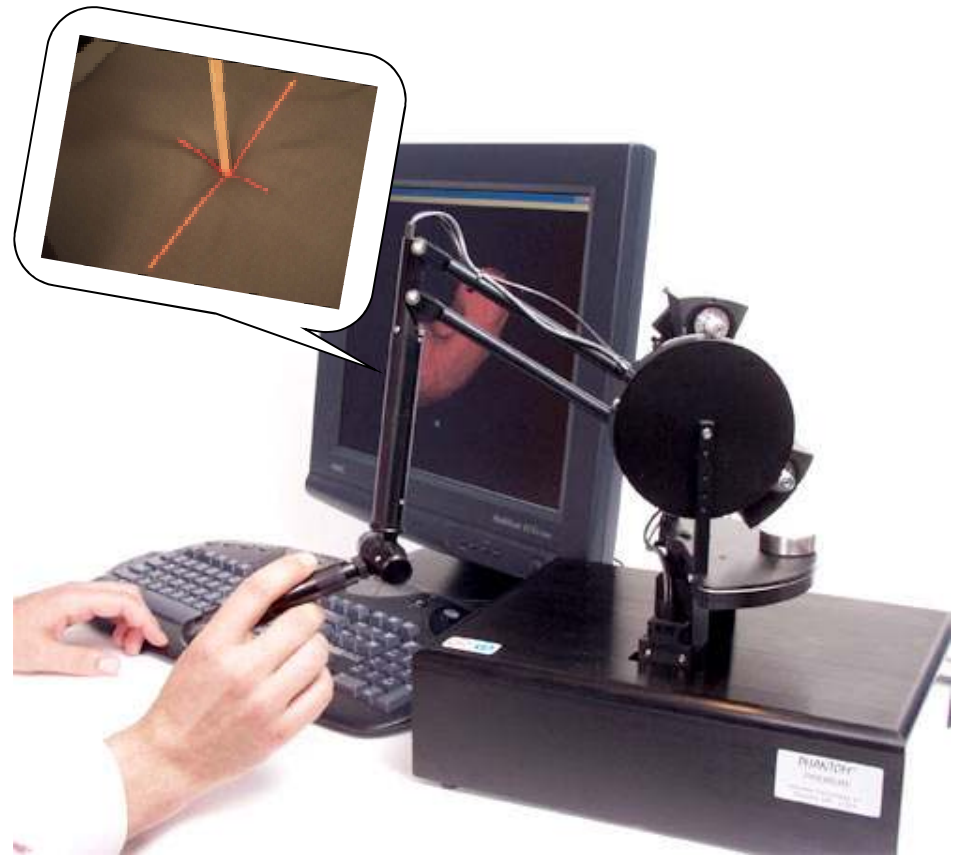


Robot arm with tendon driven compliant wrist

Haptic & Visual Telerobotic System [from E.M. Petriu, D.C. Petriu, V. Cretu, "Control System for an Interactive Programmable Robot," *Proc. CNETAC Nat. Conf. Electronics, Telecommunications, Control, and Computers*, pp. 227-235, Bucharest, Romania, Nov. 1982.]



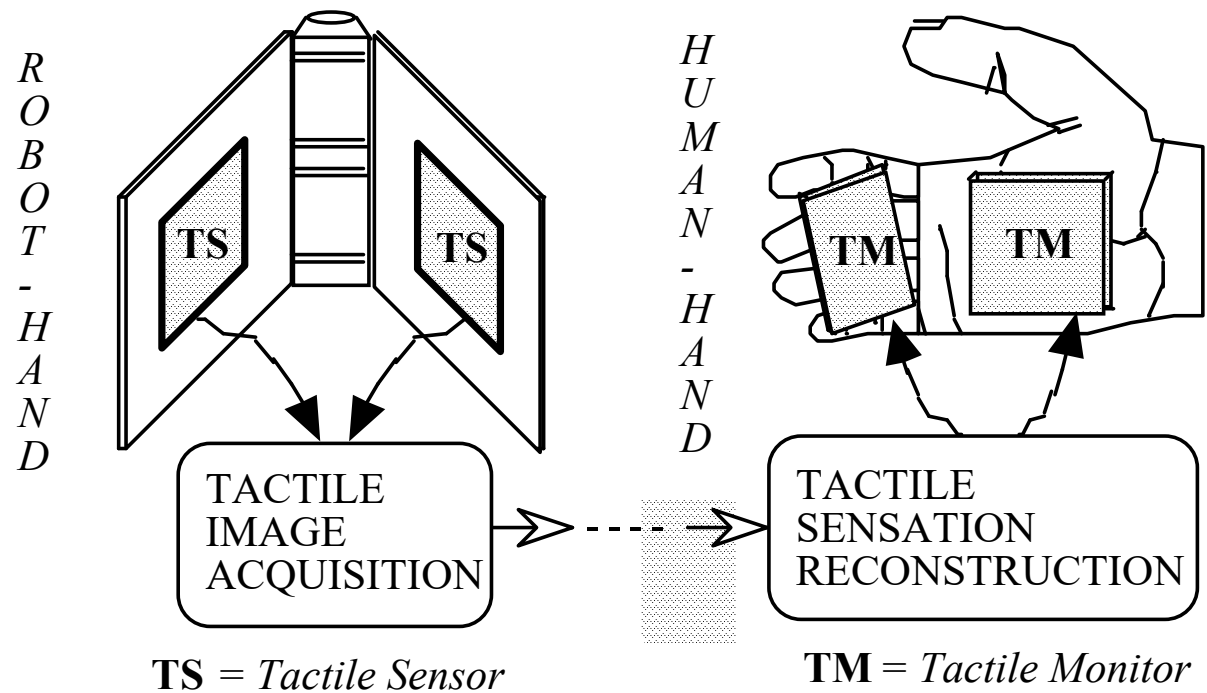
Haptic Telerobotic System: (a) the tactile probe , and (b) the tactile human feedback [from E.M. Petriu, D.C. Petriu, V. Cretu, "Control System for an Interactive Programmable Robot," *Proc. CNETAC Nat. Conf. Electronics, Telecommunications, Control, and Computers*, pp. 227-235, Bucharest, Romania, Nov. 1982.]



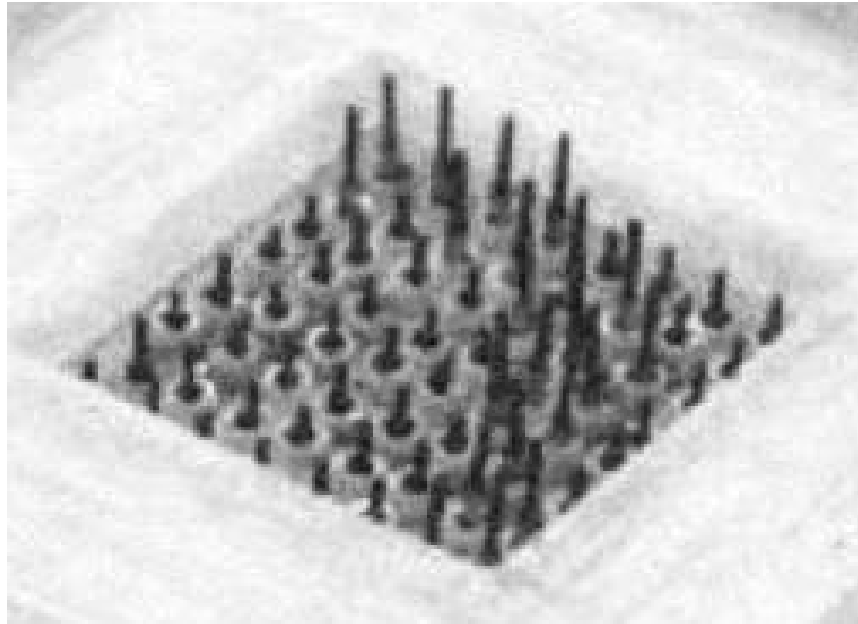
A desktop *hapto-visual human interface* allows a human teleoperator to experience the haptic feeling profiles at the point of contact as well as to see the image of a larger area around the point of contact on the explored object as captured by a video camera mounted on the robot manipulator. It includes a *PHANTOM® 6DOF* haptic device representing the **handheld replica of the probing finger** that provides the haptic feedback consisting of the 3D geometric coordinates of the point of contact measured by the laser range finder system and the force vector and torque components measured by the 6 DOF force-torque sensor at the point of contact.



Commercial “Virtual Hand Toolkit for CyberGlove/Grasp”
providing the kinesthetic human feedback interface



Haptic human interface placed on the operator's palm allows the human operator to virtually feel by touch the object profile measured by the tactile sensors placed in the jaws of the robot gripper [from E.M. Petriu, W.S. McMath, "Tactile Operator Interface for Semi-autonomous Robotic Applications," *Proc.Int. Symposium on Artificial Intell. Robotics Automat. in Space, i-SAIRS'92*, pp.77-82, Toulouse, France, 1992.]



Cutaneous tactile human interface consisting of an 8-by-8 array of vibro-tactile stimulators. The active area is 6.5 cm² (same as the tactile sensor), [from E.M. Petriu, W.S. McMath, "Tactile Operator Interface for Semi-autonomous Robotic Applications," *Proc.Int. Symposium on Artificial Intell. Robotics Automat. in Space, i-SAIRS'92*, pp.77-82, Toulouse, France, 1992.]



Tactile fingertip human interface
developed at the University of Ottawa.
It consists of miniature vibrators placed
on the fingertips. The vibrators are
individually controlled using a dynamic
model of the visco-elastic tactile sensing
mechanisms in the human fingertip.

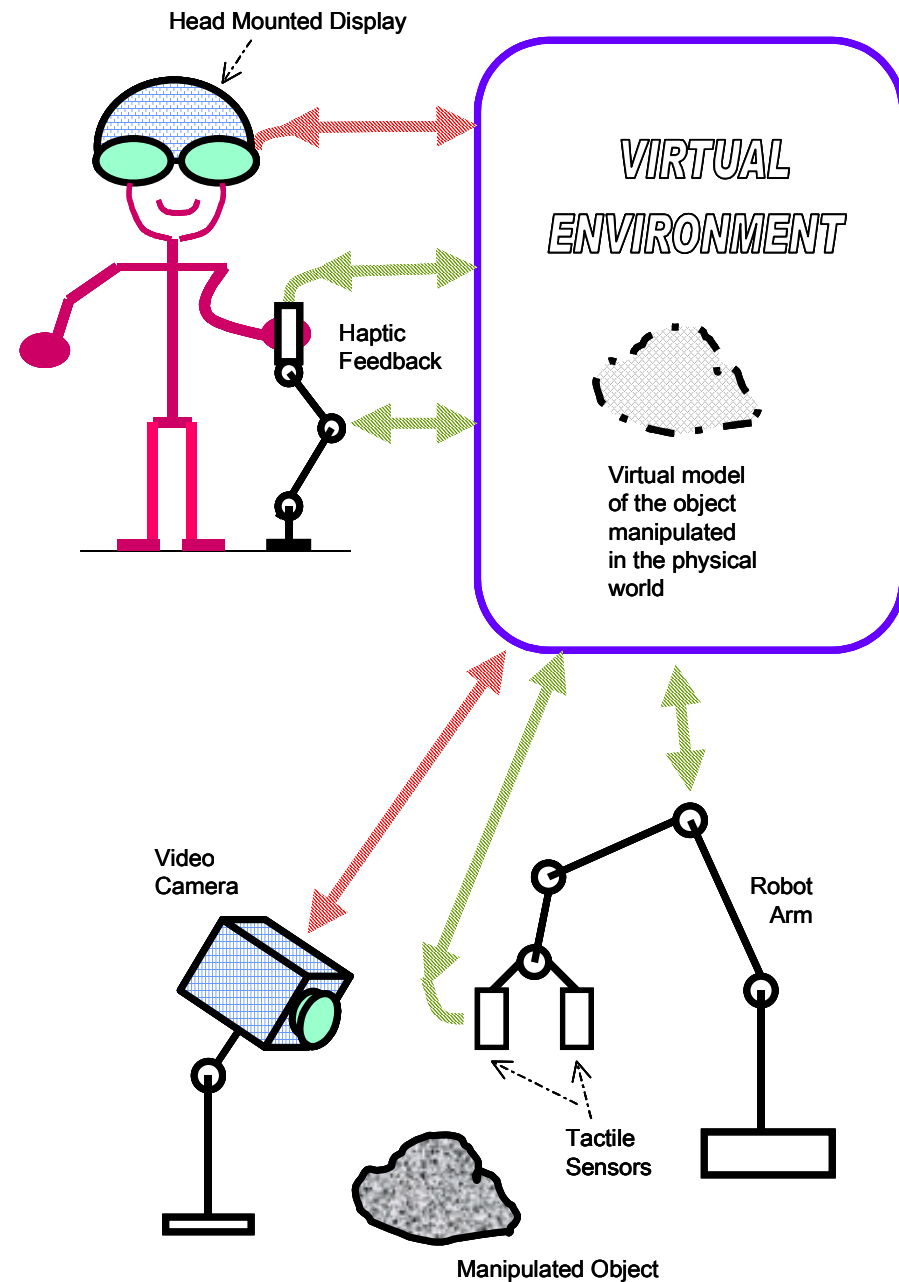


Interactive Robotic Telemanipulation

Robotic telemanipulation

is an object-oriented act which requires not only specialized *robotic hands with articulated fingers* but also *tactile, force and kinesthetic sensors* for the precise control of the forces and motions exerted on the manipulated object.

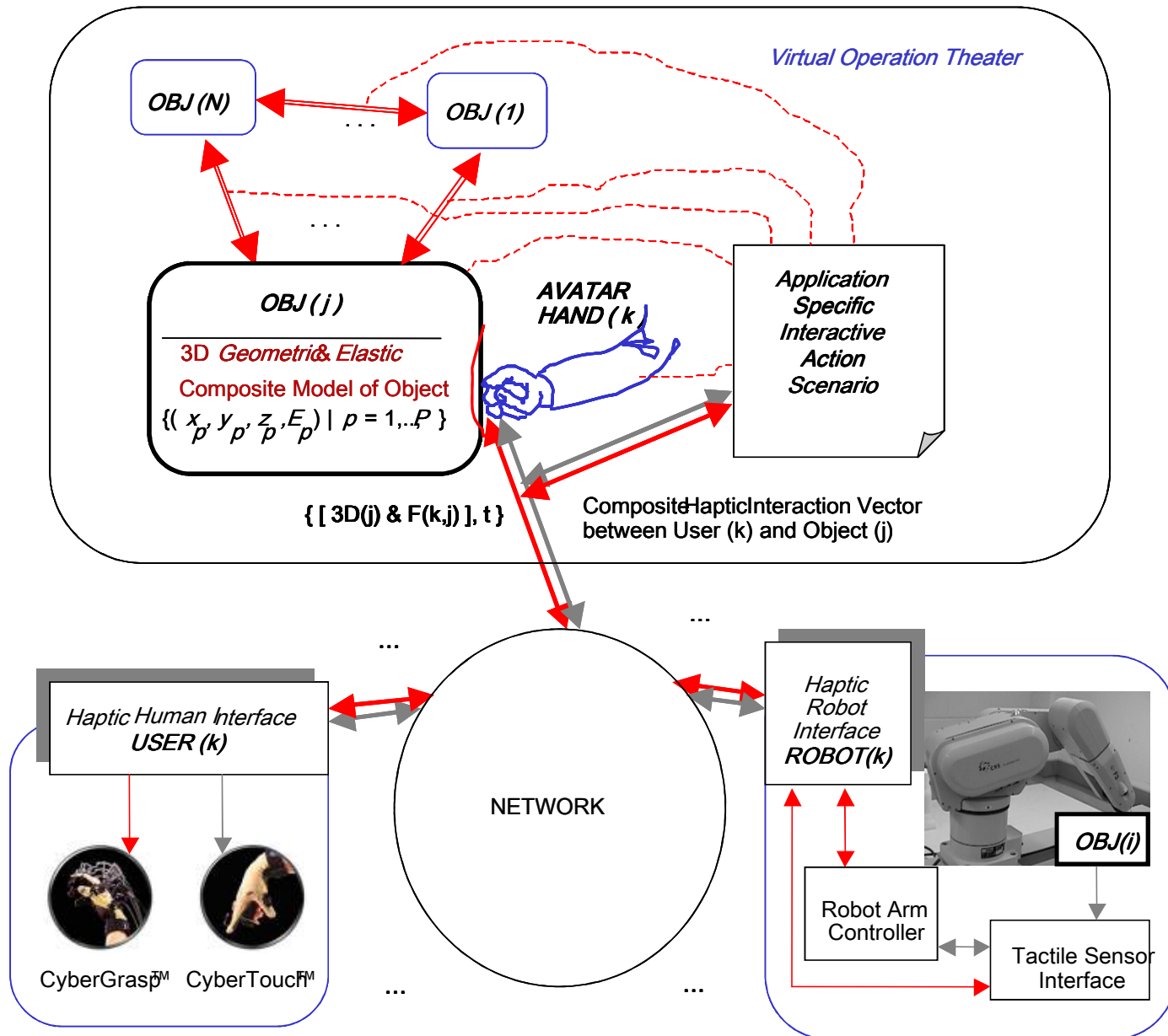
When a fully autonomous robotic dexterous manipulation is impractical in changing and unstructured environments, an alternative approach is to *combine the low-level robot computer control with the higher-level perception and task planning abilities of a human operator* equipped with adequate *human computer interfaces (HCI)*.



- ❑ **Telemanipulation systems** should have a bilateral architecture that allows a *human operator* to connect in a *transparent manner to a remote robotic manipulator*.

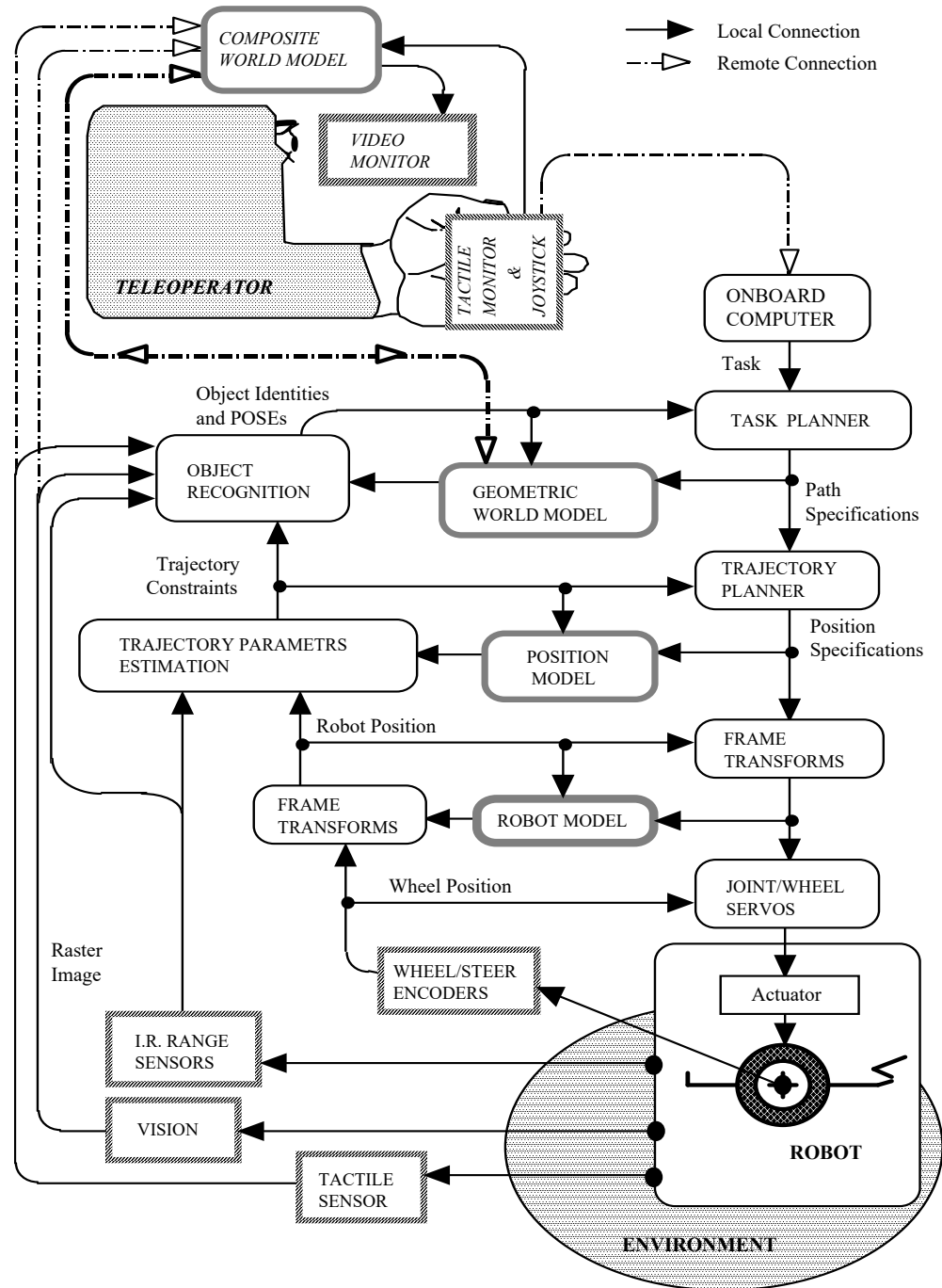
- ❑ **Human Computer Interfaces** (HCI) should provide easily perceivable and *task-related sensory displays (monitors)* which fit *naturally* the perception capabilities of the human operator.

- ❑ The potential of the emergent haptic perception technologies is significant for *applications* requiring object telemanipulation such as: (i) robot-assisted handling of materials in industry, hazardous environments, high risk security operations, or difficult to reach environments, (ii) telelearning in hands-on virtual laboratory environments for science and arts, (iii) telemedicine and medical training simulators.



Interactive Model-Based Hapto-Visual Teleoperation - a human operator equipped with haptic HCI can telemanipulate physical objects with the help of a robotic equipped with haptic sensors.

Model-based telepresence control of a robot





Canadian Space Agency:

In 1981, Canada confirmed its position as a world leader in space technology with the development of the Remote Manipulator System, or **Canadarm**.

The RMS can be used: to deploy and retrieve satellites, to hold targets, to explore samples, and to manipulate hardware for the Space Shuttle.

In 1988, Canada agreed to join the international partners to build a permanently inhabited Space Station. Canada's contribution is to design, manufacture, and operate a robotic system, the **Mobile Servicing System (MSS)**, for assembly, maintenance, and servicing tasks on the Space Station.

Vision-Based Sensing and Control for Space Robotics Applications

Michael E. Stieber, *Member, IEEE*, Michael McKay, George Vukovich, *Member, IEEE*, and Emil Petriu, *Senior Member, IEEE*

Abstract—The following problems arise in the precise positioning of payloads by space manipulators:

- 1) the precise measurement of the relative position and motion of objects in the workspace of the robot;
- 2) the design of a control system, which is robust and performs well in spite of the effects of structural flexibility and oscillations typically associated with space robots.

This paper discusses the solution to the measurement problem by a vision system using photogrammetric image processing to determine the motion of objects in real time. Performance characteristics are presented. The control problem is addressed by a new technique dealing effectively with the challenge posed by the noncollocated sensor/actuator configuration on the flexible robot structure. The laboratory implementation of the measurement and control concepts is discussed. Preliminary results validate the concepts.

Index Terms—Artificial vision, control, measurement of motion, photogrammetry, robotics.

I. INTRODUCTION

ROBOTIC systems will play an important role in reducing hazards and increasing productivity of humans in space. A prime example is the Mobile Servicing System (MSS) shown in Fig. 1 which is presently being developed by the Canadian Space Agency for the assembly and external maintenance of the International Space Station (ISS) [1]. As the tasks performed by space robots become more complex, the need for more human-like characteristics emerges. As with humans, the sense of sight is essential to enabling efficient interaction with the environment. More important than the sense of sight per se is the ability to process images in such a way as to enable more efficient, accurate and autonomous control of the robot.

This paper addresses measurement and control problems associated with the precise positioning of large space robot manipulators like the Space Station Remote Manipulator System (SSRMS) shown in Fig. 1, which typically have a very high payload-to-manipulator mass ratio (e.g. 116 000 kg/1500 kg for SSRMS) and relatively low stiffness, resulting in highly time-variant dynamic behavior with significant low-frequency oscillations. A theoretical concept for the systematic design of an instrumentation architecture for such systems

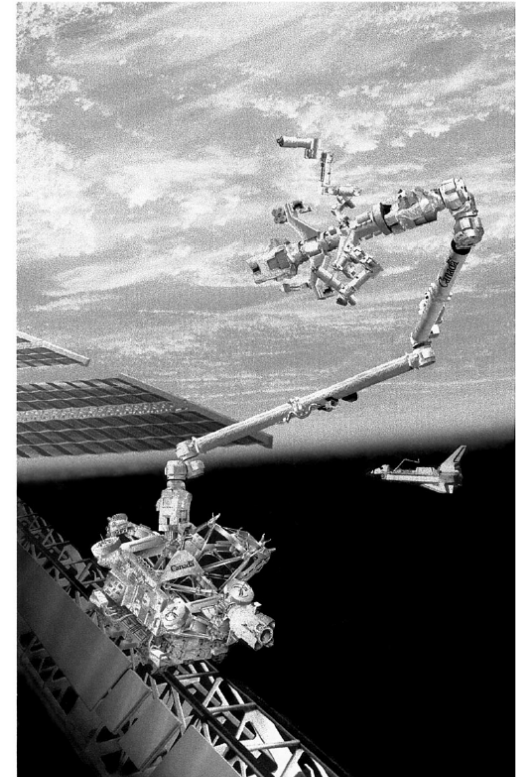


Fig. 1. Mobile Servicing System on the International Space Station.

was presented in [2]. This paper discusses the experimental implementation and evaluation of this concept in a laboratory setting. Section II discusses the measurement of the manipulator payload motion, including the contributions due to structural flexibility, relative to other objects in the manipulator workspace using a vision system. In Section III we extend the theoretical concept of [2] to the case of partially noncollocated sensor/actuator configurations on flexible structures and discuss the design and performance of a control system for the laboratory robot.

Manuscript received May 23, 1996; revised April 12, 1999.

M. E. Stieber and G. Vukovich are with the Canadian Space Agency, St. Hubert, P.Q., Canada.

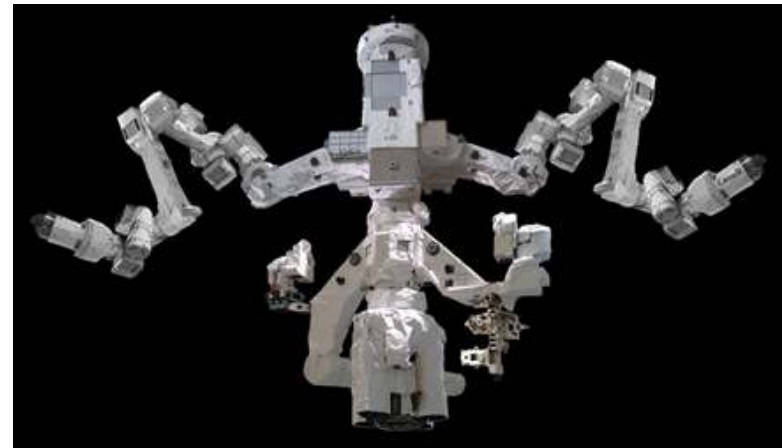
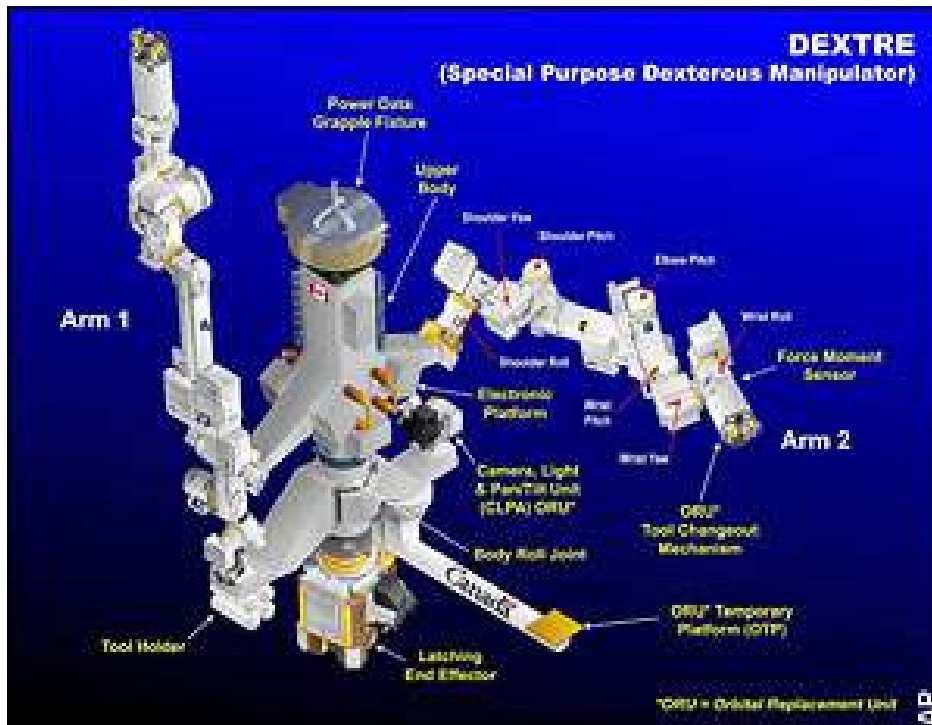
M. McKay is with the Department of National Defense, Ottawa, Ont., Canada.

E. Petriu is with the University of Ottawa, Ottawa, Ont., K1N 6N5, Canada. Publisher Item Identifier S 0018-9456(99)06676-0.

Canadian space robot 'Dextre' a high-tech marvel

Updated Mon. Mar. 10 2008 8:35 AM ET CTV.ca News Staff

,,, Dextre the robot will be the latest Canadian-built addition to the International Space Station. "Dextre is the second arm for the station built by Canada," astronaut Steve Swanson told Canada AM on Monday from Cape Canaveral. "And its task is to do jobs that are more of a fine, finesse manipulator-type activity. Usually we would do spacewalks to change out components that have broken on the station. But now with Dextre, we can do that from inside and use Dextre's arms to do things that a human could do."



<http://www.ctv.ca/mar/static/dextre/>

Da Vinci Surgical System is a robotic surgical system made by the American company Intuitive Surgical. Approved by the Food and Drug Administration (FDA) in 2000, it is designed to facilitate complex surgery using a minimally invasive approach, and is controlled by a surgeon from a console.

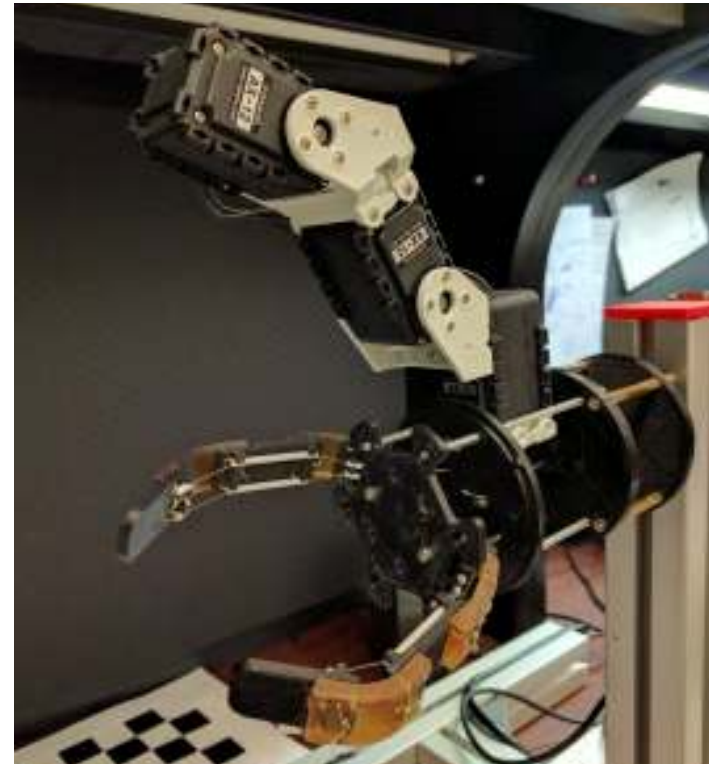


Da Vinci System allows the surgeon's hand movements to be translated into smaller, precise movements of tiny instruments inside the patient's body.

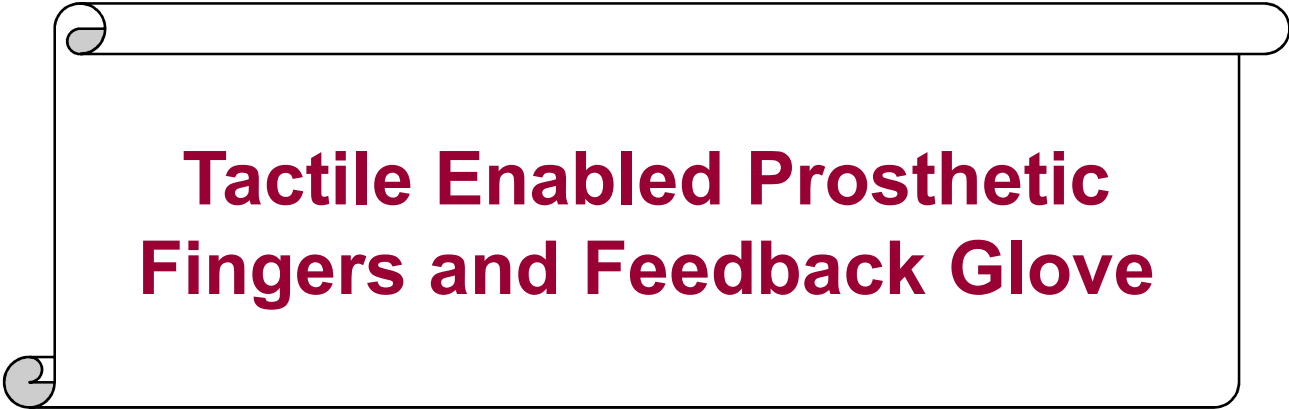
As of June 30, 2014, there were installed 3,102 units worldwide. an estimated 200,000 surgeries conducted in 2012

Multi-Finger Dexterous Robot Hand

Vision, tactile, and flex joint sensors allow tracking finger phalanges' position, provide information of the object's unknown orientation for in-hand manipulation by **the two -finger underactuated hand with a fully-actuated intelligent thumb** capable of trajectory planning. A *fuzzy logic controller* allows to obtain a stable grasp After grasp, the manipulate object can be reoriented by the thumb taking advantage of the compliance of the flex joint fingers



[from V. Prado da Fonseca, D.J. Kucherhan, T. E. Alves de Oliveira, D. Zhi, E.M. Petriu "Fuzzy Controlled Object Manipulation using a Three-Fingered Robotic Hand," 10th Annual IEEE Int. Systems Conference - SysCon 2017, pp. 346 - 351, Montreal, Que, April 2017].



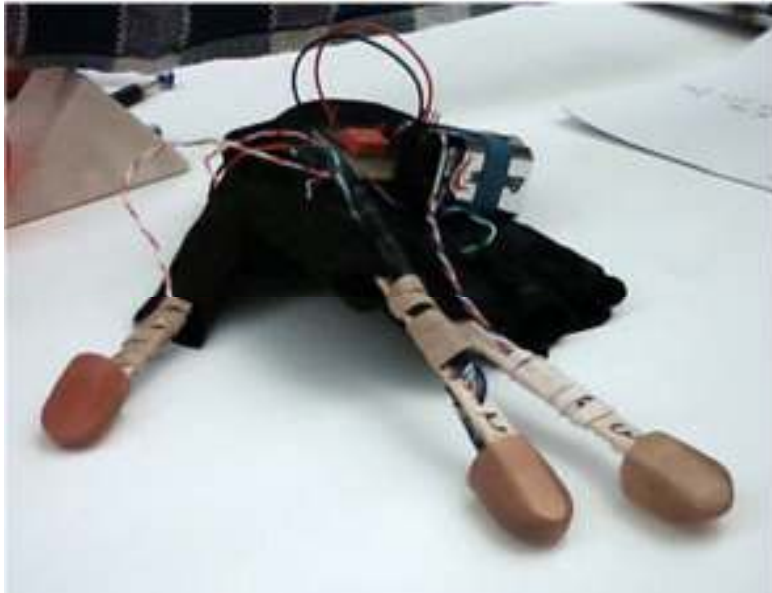
**Tactile Enabled Prosthetic
Fingers and Feedback Glove**



Tactile Enabled Prosthetic fingertip:

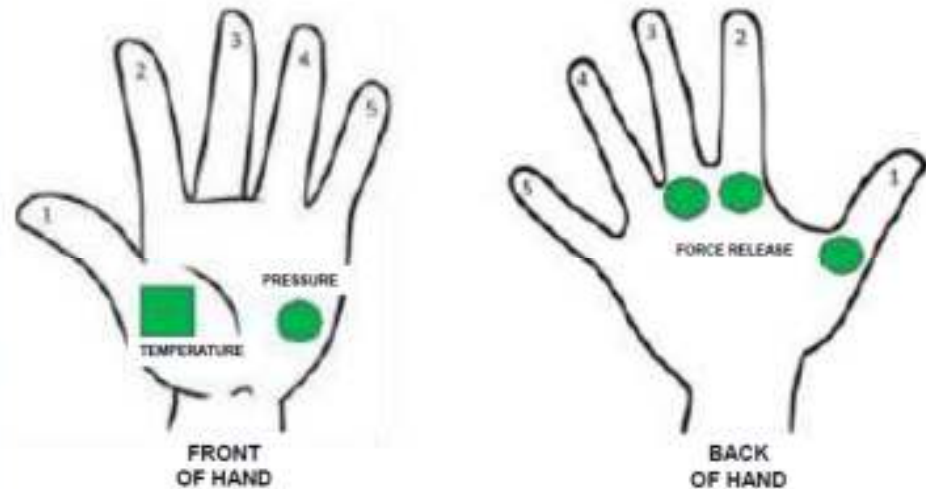
- four *force sensors* embedded in the fingertip: one *force sensing resistor* measuring exerted force amplitude (0.1 N - 20 N), and three *thin pot* sensors measuring the relative position of the force (0.7 N- 2.2 N);
- *piezoelectric vibration sensor* measuring subtle vibrational patterns;
- digital *temperature sensor* (-10°C to +85°C, thermal gradient < 0.1 °C)

[from D. J. Kucherhan, M. Goubran, V. Prado da Fonseca, T.E. Alves de Oliveira, E.M. Petriu, V. Groza, "Object Recognition Through Manipulation Using Tactile Enabled Prosthetic Fingers and Feedback Glove - Experimental Study," 2018 IEEE International Symposium on Medical Measurements & Applications (MeMeA) Rome, Italy, June 2018].



Tactile-enabled assistive glove

with three prosthetic fingers conveys multimodal tactile feedback to human operator's hand while she/he performs dexterous object manipulation and recognition. A Peltier thermoelectric tile provides *thermal feedback*. Linear Resonant Actuators generate *force and vibration feedback*.



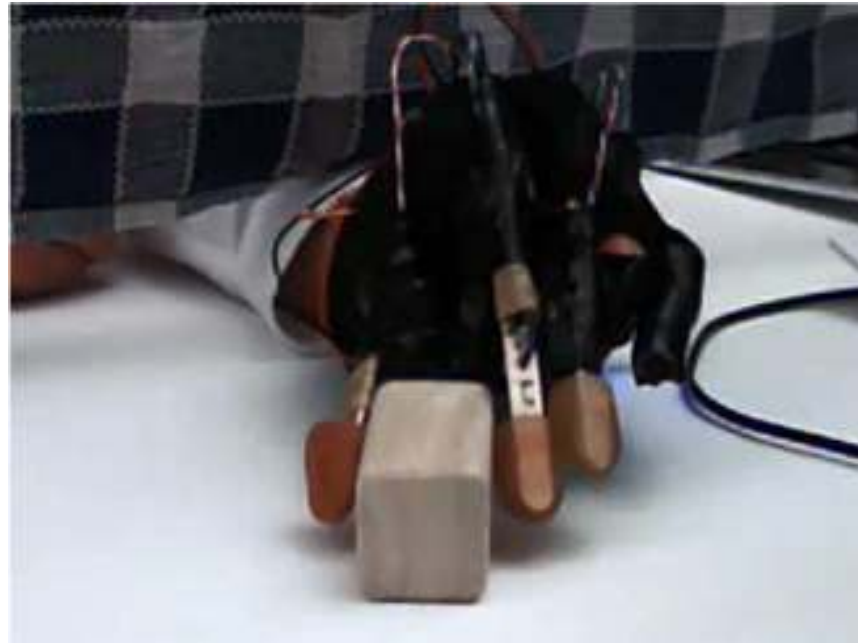
Placement of the tactile actuators in the assistive glove:

[from D. J. Kucherhan, M. Goubran, V. Prado da Fonseca, T.E. Alves de Oliveira, E.M. Petriu, V. Groza, "Object Recognition Through Manipulation Using Tactile Enabled Prosthetic Fingers and Feedback Glove - Experimental Study," 2018 IEEE International Symposium on Medical Measurements & Applications (MeMeA) Rome, Italy, June 2018].

Human subject exploring an object behind a fabric screen

* The subject puts on the glove so that the three artificial fingers were secured to their natural fingers, tape was wrapped around the length of subject's gloved fingers to mask the natural mechanoreceptors within each subject's finger.

* Directly in front of the subject was the *map of the tactile actuators in the assistive glove* to be used to orally identify the sensations felt whilst using the glove.



[from D. J. Kucherhan, M. Goubran, V. Prado da Fonseca, T.E. Alves de Oliveira, E.M. Petriu, V. Groza, "Object Recognition Through Manipulation Using Tactile Enabled Prosthetic Fingers and Feedback Glove - Experimental Study," 2018 IEEE International Symposium on Medical Measurements & Applications (MeMeA) Rome, Italy, June 2018].

During the **active touch** portion each human-subjects was asked to conduct three experiments aiming to identify a mystery object within the concealed experiment area. Subjects were allowed unlimited time to identify the mystery object.



← **Objects used for active touch experiments** (pen used for scale):

Two experiments used mystery *objects that were common for every subject*: the plastic toy alligator (item 1) and the wooden triangular block (item 12).

For the third experiment, subjects were provided a mystery object which was randomly selected from the 22 different objects by one of the researchers.

[from D. J. Kucherhan, M. Goubran, V. Prado da Fonseca, T.E. Alves de Oliveira, E.M. Petriu, V. Groza, "Object Recognition Through Manipulation Using Tactile Enabled Prosthetic Fingers and Feedback Glove - Experimental Study," 2018 IEEE International Symposium on Medical Measurements & Applications (MeMeA) Rome, Italy, June 2018].

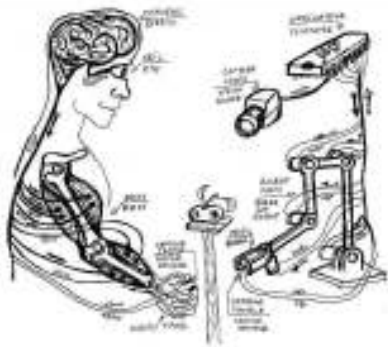
Mystery object #1, common to all subjects, was the plastic alligator. Only two of the five subjects were able to correctly identify it. Overall success rate of 40%.

Mystery object #2, common to all subjects, was the wooden triangular prism. Only two of the five subjects were able to correctly identify it. Overall success rate of 40%.

Mystery object #3 was a randomly selected object for each subject. The overall success rate was 60%.

Active Touch	Subject 1	Subject 2	Subject 3	Subject 4	Subject 5
Mystery Object # 3	Teddy bear	Tiara	Tiara	Frog	Teddy bear
Identified Object	Cow	Tiara	Brain	Frog	Teddy bear
	x	✓	x	✓	✓

[from D. J. Kucherhan, M. Goubran, V. Prado da Fonseca, T.E. Alves de Oliveira, E.M. Petriu, V. Groza, "Object Recognition Through Manipulation Using Tactile Enabled Prosthetic Fingers and Feedback Glove - Experimental Study," 2018 IEEE International Symposium on Medical Measurements & Applications (MeMeA) Rome, Italy, June 2018].



Thank You!